(Applied BioSystems) were performed as previously described [61]. Expression levels were all normalized against β-ACTIN. The relative level of each gene expression were generated from the undifferentiated H9 hES cell or 201B7 hiPS cells cultured on mitomycin-inactivated mouse embryonic fibroblasts (MEF) in KSR-based medium (Sample No. 1–2). Heat-map colors (red for up-regulation, blue for down-regulation) depict gene expression. (**C**) Teratomas derived from H9 hES cells at passage 44 or 201B7 iPS cells at passage 26 maintained in $hESF9a_{2i}$ conditions.
(TIF)

Table S1 The composition of media used for serum-free culture. * The composition of the basal medium, ESF for culturing mouse ES cells, is described in Furue et al., 2005 [22]. ** hESF9 medium is described in Furue et al., 2008 [8]. *** hESF9a medium is described in Hayashi and Furue et al., 2010 [23].
(DOC)

Table S2 A list of the used antibodies.
(DOC)

Table S3 A list of the used primers for RT-PCR.
(DOC)

Table S4 A list of the used primers for qRT-PCR and siRNAs.
(DOC)

Acknowledgments

We thank Prof. Peter W. Andrews (University of Sheffield, Sheffield, UK) for the valuable comments on the manuscript and generous gift of anti-SSEA-4, A2B5, and Tra-2-54 antibodies, Dr. Jie Na (Tsinghua University, Beijing, China) for the valuable comments and discussions on the manuscript, Dr. Ivana Barbaric (University of Sheffield) for the valuable comments on the manuscript, Dr. Takeshi Tomonaga (National Institute of Biomedical Innovation) for the technical advices, and Dr. Hiroshi Takemori (National Institute of Biomedical Innovation) for the generous gift of the chemical library. We also thank Ayaka Fujiki, Mari Wakabayashi, Naoko Ueda, Akiko Hamada, Yujung Liu, Hiroko Ochi, Eiko Kawaguchi, Midori Hayashida, Yutaka Ozawa, Azusa Ohtani, and Setsuko Shioda for excellent technical support and Dr. J. Denry Sato for editorial assistance.

Author Contributions

Conceived and designed the experiments: MK MKF. Performed the experiments: MK SK DT MS HM SM NH MH KUY AK KY. Analyzed the data: MK. Wrote the paper: MK MKF.

References

1. Vallier L, Reynolds D, Pedersen RA (2004) Nodal inhibits differentiation of human embryonic stem cells along the neuroectodermal default pathway. Dev. Biol. 275: 403–421.
2. Vallier L, Alexander M, Pedersen RA (2005) Activin/Nodal and FGF pathways cooperate to maintain pluripotency of human embryonic stem cells. J Cell Science 118: 4495–4509.
3. James D, Levine AJ, Besser D, Hemmati-Brivanlou A (2005) TGFβ/activin/nodal signaling is necessary for the maintenance of pluripotency in human embryonic stem cells. Development 132: 1273–1282.
4. Pebay A, Wong RC, Pitson SM, Wolvetang EJ, Peh GS, et al. (2005) Essential roles of sphingosine-1-phosphate and platelet-derived growth factor in the maintenance of human embryonic stem cells. Stem Cells 23: 1541–1548.
5. Bendall SC, Stewart MH, Menendez P, George D, Vijayaragavan K, et al. (2007) IGF and FGF cooperatively establish the regulatory stem cell niche of pluripotent human cells in vitro. Nature 448: 1015–1021.
6. Dvorak P, Dvorakova D, Koskova S, Vodinska M, Najvirtova M, et al. (2005) Expression and potential role of fibroblast growth factor 2 and its receptors in human embryonic stem cells. Stem Cells 23: 1200–1211.
7. Avery S, Inniss K, Moore H (2006) The regulation of self-renewal in human embryonic stem cells. Stem Cells Dev. 15: 729–740.
8. Furue MK, Na J, Jackson JP, Okamoto T, Jones M, et al. (2008) Heparin promotes the growth of human embryonic stem cells in a defined serum-free medium. PNAS 105: 13409–13414.
9. Ding VM, Boersema PJ, Foong LY, Preisinger C, Koh G, et al. (2011) Tyrosine phosphorylation profiling in FGF-2 stimulated human embryonic stem cells. PLoS One 6: e17538.
10. Amit M, Carpenter MK, Inokuma MS, Chiu CP, Harris CP, et al. (2000) Clonally derived human embryonic stem cell lines maintain pluripotency and proliferative potential for prolonged periods of culture. Developmental Biology 227: 271–278.
11. Hoffman LM, Carpenter MK (2005) Characterization and culture of human embryonic stem cells. Nat. Biotechnol. 23: 699–708.
12. Xu RH, Peck RM, Li DS, Feng X, Ludwig T, et al. (2005) Basic FGF and suppression of BMP signaling sustain undifferentiated proliferation of human ES cells. Nat. Methods 2: 185–190.
13. Schlessinger J (2004) Common and distinct elements in cellular signaling via EGF and FGF receptors. Science 306: 1506–1507.
14. Dreesen O, Brivanlou AH (2007) Signaling pathways in cancer and embryonic stem cells. Stem Cell Rev. 3: 7–17.
15. Armstrong L, Hughes O, Yung S, Hyslop L, Stewart R, et al. (2006) The role of PI3K/AKT, MAPK/ERK and NFκβ signalling in the maintenance of human embryonic stem cell pluripotency and viability highlighted by transcriptional profiling and functional analysis. Hum. Mol. Genet. 15: 1894–1913.
16. Eiselleova L, Matulka K, Kriz V, Kunova M, Schmidtova Z, et al. (2009) A complex role for FGF-2 in self-renewal, survival, and adhesion of human embryonic stem cells. Stem Cells 27: 1847–1857.
17. Ding VM, Ling L, Natarajan S, Yap MG, Cool SM, et al. (2010) FGF-2 modulates Wnt signaling in undifferentiated hESC and iPS cells through activated PI3-K/GSK3β signaling. J. Cell Physiol. 225: 417–428.
18. Na J, Furue MK, Andrews PW (2010) Inhibition of ERK1/2 prevents neural and mesendodermal differentiation and promotes human embryonic stem cell self-renewal. Stem Cell Research 5: 157–169.
19. Nakanishi M, Kurisaki A, Hayashi Y, Warashina M, Ishiura S, et al. (2009) Directed induction of anterior and posterior primitive streak by Wnt from embryonic stem cells cultured in a chemically defined serum-free medium. FASEB Journal 23: 114–122.
20. Aihara Y, Hayashi Y, Hirata M, Ariki N, Shibata S, et al. (2010) Induction of neural crest cells from mouse embryonic stem cells in a serum-free monolayer culture. International Journal of Developmental Biology 54: 1287–1294.
21. Kusuda Furue M, Tateyama D, Kinehara M, Na J, Okamoto T, et al. (2010) Advantages and difficulties in culturing human pluripotent stem cells in growth factor-defined serum-free medium. In Vitro Cellular and Developmental Biology Animal 46: 573–576.
22. Furue M, Okamoto T, Hayashi Y, Okochi H, Fujimoto M, et al. (2005) Leukemia inhibitory factor as an anti-apoptotic mitogen for pluripotent mouse embryonic stem cells in a serum-free medium without feeder cells. In Vitro Cellular and Developmental Biology Animal 41: 19–28.
23. Hayashi Y, Chan T, Warashina M, Fukuda M, Ariizumi T, et al. (2010) Reduction of N-glycolylneuraminic acid in human induced pluripotent stem cells generated or cultured under feeder- and serum-free defined conditions. PLoS One 5: e14099.
24. Watanabe K, Ueno M, Kamiya D, Nishiyama A, Matsumura M, et al. (2007) A ROCK inhibitor permits survival of dissociated human embryonic stem cells. Nat. Biotechnol. 25: 681–686.
25. Wang X, Lin G, Martins-Taylor K, Zeng H, Xu RH (2009) Inhibition of caspase-mediated anoikis is critical for basic fibroblast growth factor-sustained culture of human pluripotent stem cells. J Biol. Chem. 284: 34054–34064.
26. Takahashi K, Tanabe K, Ohnuki M, Narita M, Ichisaka T, et al. (2007) Induction of pluripotent stem cells from adult human fibroblasts by defined factors. Cell 131: 861–872.
27. Lyssiotis CA, Foreman RK, Staerk J, Garcia M, Mathur D, et al. (2009) Reprogramming of murine fibroblasts to induced pluripotent stem cells with chemical complementation of Klf4. PNAS 106: 8912–8917.
28. Barbaric I, Gokhale PJ, Jones M, Glen A, Baker D, et al. (2010) Novel regulators of stem cell fates identified by a multivariate phenotype screen of small compounds on human embryonic stem cell colonies. Stem Cell Research 5: 104–119.
29. Martiny-Baron G, Kazanietz MG, Mischak H, Blumberg PM, Kochs G, et al. (1993) Selective inhibition of protein kinase C isozymes by the indolocarbazole Gö 6976. J Biol. Chem. 268: 9194–9197.
30. Damoiseaux R, Sherman SP, Alva JA, Peterson C, Pyle AD (2009) Integrated chemical genomics reveals modifiers of survival in human embryonic stem cells. Stem Cells 27: 533–542.
31. Thomson JA, Itskovitz-Eldor J, Shapiro SS, Waknitz MA, Swiergiel JJ, et al. (1998) Embryonic stem cell lines derived from human blastocysts. Science 282: 1145–1147.
32. Boersema PJ, Foong LY, Ding VM, Lemeer S, van Breukelen B, et al. (2010) In-depth qualitative and quantitative profiling of tyrosine phosphorylation using a combination of phosphopeptide immunoaffinity purification and stable isotope dimethyl labeling. Mol. Cell Proteomics 9: 84–99.

33. Nishino K, Toyoda M, Yamazaki-Inoue M, Fukawatase Y, Chikazawa E, et al. (2011) DNA methylation dynamics in human induced pluripotent stem cells over time. PLoS Genet 7: e1002085.
34. Kannagi R, Cochran NA, Ishigami F, Hakomori S, Andrews PW, et al. (1983) Stage-specific embryonic antigens (SSEA-3 and -4) are epitopes of a unique globo-series ganglioside isolated from human teratocarcinoma cells. EMBO Journal 2: 2355–2361.
35. Andrews PW, Banting G, Damjanov I, Arnaud D, Avner P (1984) Three monoclonal antibodies defining distinct differentiation antigens associated with different high molecular weight polypeptides on the surface of human embryonal carcinoma cells. Hybridoma 3: 347–361.
36. Draper JS, Pigott C, Thomson JA, Andrews PW (2002) Surface antigens of human embryonic stem cells: changes upon differentiation in culture. Journal of Anatomy 200: 249–258.
37. Solter D, Knowles BB (1978) Monoclonal antibody defining a stage-specific mouse embryonic antigen (SSEA-1). PNAS 75: 5565–5569.
38. Nishizuka Y (1995) Protein kinase C and lipid signaling for sustained cellular responses. FASEB J. 9: 484–496.
39. Newton AC (1997) Regulation of protein kinase C. Curr. Opin. Cell Biol. 9: 161–167.
40. Mochly-Rosen D, Gordon AS (1998) Anchoring proteins for protein kinase C: a means for isozyme selectivity. FASEB J. 12: 35–42.
41. Goode N, Hughes K, Woodgett JR, Parker PJ (1992) Differential regulation of glycogen synthase kinase-3β by protein kinase C isotypes. J Biol. Chem. 267: 16878–16882.
42. Kaidanovich-Beilin O, Woodgett JR (2011) GSK-3: Functional Insights from Cell Biology and Animal Models. Front. Mol. Neurosci. 4: 40.
43. Fang X, Yu S, Tanyi JL, Lu Y, Woodgett JR, et al. (2002) Convergence of multiple signaling cascades at glycogen synthase kinase 3: Edg receptor-mediated phosphorylation and inactivation by lysophosphatidic acid through a protein kinase C-dependent intracellular pathway. Mol. Cell. Biol. 22: 2099–2110.
44. Chen S, Borowiak M, Fox JL, Maehr R, Osafune K, et al. (2009) A small molecule that directs differentiation of human ESCs into the pancreatic lineage. Nat. Chem Biol. 5: 258–265.
45. Feng X, Zhang J, Smuga-Otto K, Tian S, Yu J, et al. (2012) Protein Kinase C Mediated Extraembryonic Endoderm Differentiation of Human Embryonic Stem Cells. Stem Cells 30:461–470.
46. Chou MM, Hou W, Johnson J, Graham LK, Lee MH, et al. (1998) Regulation of protein kinase C ζ by PI 3-kinase and PDK-1. Curr. Biol. 8: 1069–1077.
47. Doornbos RP, Theelen M, van der Hoeven PC, van Blitterswijk WJ, Verkleij AJ, et al. (1999) Protein kinase Cζ is a negative regulator of protein kinase B activity. J Biol. Chem. 26: 8589–8596.
48. Dutta D, Ray S, Home P, Larson M, Wolfe MW, et al. (2011) Self-Renewal Versus Lineage Commitment of Embryonic Stem Cells:Protein Kinase C Signaling Shifts the Balance. Stem Cells 29: 618–628.
49. Moon RT, Kohn AD, De Ferrari GV, Kaykas A (2004) WNT and β-catenin signalling: diseases and therapies. Nat. Rev. Genet. 5: 691–701.
50. Sato N, Meijer L, Skaltsounis L, Greengard P, Brivanlou AH (2004) Maintenance of pluripotency in human and mouse embryonic stem cells through activation of Wnt signaling by a pharmacological GSK-3-specific inhibitor. Nat. Medicine 10: 55–63.
51. Dravid G, Ye Z, Hammond H, Chen G, Pyle A, et al. (2005) Defining the role of Wnt/β-catenin signaling in the survival, proliferation, and self-renewal of human embryonic stem cells. Stem Cells 23: 1489–1501.
52. Cai L, Ye Z, Zhou BY, Mali P, Zhou C, et al. (2007) Promoting human embryonic stem cell renewal or differentiation by modulating Wnt signal and culture conditions. Cell Research 17: 62–72.
53. Sumi T, Tsuneyoshi N, Nakatsuji N, Suemori H (2008) Defining early lineage specification of human embryonic stem cells by the orchestrated balance of canonical Wnt/β-catenin, Activin/Nodal and BMP signaling. Development 135: 2969–2979.
54. Vallier L, Mendjan S, Brown S, Chng Z, Teo A, et al. (2009) Activin/Nodal signalling maintains pluripotency by controlling Nanog expression. Development 136: 1339–1349.
55. Ying QL, Nichols J, Chambers I, Smith A (2003) BMP induction of Id proteins suppresses differentiation and sustains embryonic stem cell self-renewal in collaboration with STAT3. Cell 115: 281–292.
56. Chen L, Hahn H, Wu G, Chen CH, Liron T, et al. (2001) Opposing cardioprotective actions and parallel hypertrophic effects of δPKC and εPKC. PNAS 98: 11114–11119.
57. Brandman R, Disatnik MH, Churchill E, Mochly-Rosen D (2007) Peptides derived from the C2 domain of protein kinase Cε (εPKC) modulate εPKC activity and identify potential protein-protein interaction surfaces. J Biol. Chem. 282: 4113–4123.
58. Toyoda M, Yamazaki-Inoue M, Itakura Y, Kuno A, Ogawa T, et al. (2011) Lectin microarray analysis of pluripotent and multipotent stem cells. Genes Cells 16: 1–11.
59. Okamoto R, Suemori H, Nakatsuji N, Nito S, Kondo Y, et al. (2004) Development of A Novel Measuring Method for Alkaline Phosphatase Activity of Primate Embryonic Stem Cell. Tissue culture research communications : the journal of experimental & applied cell culture research 23: 36.
60. Hayashi Y, Furue MK, Okamoto T, Ohnuma K, Myoishi Y, et al. (2007) Integrins regulate mouse embryonic stem cell self-renewal. Stem Cells 25: 3005–3015.
61. Adewumi O, Aflatoonian B, Ahrlund-Richter L, Amit M, Andrews PW, et al. (2007) Characterization of human embryonic stem cell lines by the International Stem Cell Initiative. Nat. Biotechnol. 25: 803–816.
62. Chia NY, Chan YS, Feng B, Lu X, Orlov YL, et al. (2010) A genome-wide RNAi screen reveals determinants of human embryonic stem cell identity. Nature 468: 316–320.

Glycobiology vol. 23 no. 3 pp. 322–336, 2013
doi:10.1093/glycob/cws159
Advance Access publication on November 15, 2012

A novel antibody for human induced pluripotent stem cells and embryonic stem cells recognizes a type of keratan sulfate lacking oversulfated structures

Keiko Kawabe[2,3], Daiki Tateyama[3], Hidenao Toyoda[4], Nana Kawasaki[5], Noritaka Hashii[5], Hiromi Nakao[2], Shogo Matsumoto[2], Motohiro Nonaka[2,†], Hiroko Matsumura[3], Yoshinori Hirose[4], Ayaha Morita[4], Madoka Katayama[6], Makoto Sakuma[6], Nobuko Kawasaki[2], Miho Kusuda Furue[3], and Toshisuke Kawasaki[1,2]

[2]Research Center for Glycobiotechnology, Ritsumeikan University, Noji-Higashi, 1-1-1, Kusatsu, Shiga 525-8577, Japan; [3]Laboratory of Stem Cell Cultures, Department of Disease Bioresources, National Institute of Biomedical Innovation, Ibaraki, Osaka 567-0085, Japan; [4]Laboratory of Bio-analytical Chemistry, Faculty of Pharmaceutical Sciences, Ritsumeikan University, Shiga 525-8577, Japan; [5]Division of Biological Chemistry and Biologicals, National Institute of Health Sciences, Tokyo 158-8501, Japan; and [6]Biologicals Group, Research and Development Department, Seikagaku Biobusiness Corporation, Tokyo 207-0021, Japan

Received on August 19, 2012; revised on October 26, 2012; accepted on November 2, 2012

We have generated a monoclonal antibody (R-10G) specific to human induced pluripotent stem (hiPS)/embryonic stem (hES) cells by using hiPS cells (Tic) as an antigen, followed by differential screening of mouse hybridomas with hiPS and human embryonal carcinoma (hEC) cells. Upon western blotting with R-10G, hiPS/ES cell lysates gave a single but an unusually diffuse band at a position corresponding to >250 kDa. The antigen protein was isolated from the induced pluripotent stem (iPS) cell lysates with an affinity column of R-10G. The R-10G positive band was resistant to digestion with peptide *N*-glycanase F (PNGase F), neuraminidase, fucosidase, chondrotinase ABC and heparinase mix, but it disappeared almost completely on digestion with keratanase, keratanase II and endo-β-galactosidase, indicating that the R-10G epitope is a keratan sulfate. The carrier protein of the R-10G epitope was identified as podocalyxin by liquid chromatography/mass spectrometry (LC/MS/MS) analysis of the R-10G positive-protein band material obtained on sodium dodecyl sulfate–polyacrylamide gel electrophoresis (SDS-PAGE). The R-10G epitope is a type of keratan sulfate with some unique properties. (1) The epitope is expressed only on hiPS/ES cells, i.e. not on hEC cells, unlike those recognized by the conventional hiPS/ES marker antibodies. (2) The epitope is a type of keratan sulfate lacking oversulfated structures and is not immunologically cross-reactive with high-sulfated keratan sulfate. (3) The R-10G epitope is distributed heterogeneously on hiPS cells, suggesting that a single colony of undifferentiated hiPS cells consists of different cell subtypes. Thus, R-10G is a novel antibody recognizing hiPS/ES cells, and should be a new molecular probe for disclosing the roles of glycans on these cells.

Keywords: embryonic stem cells / induced pluripotent stem cells / keratan sulfate / monoclonal antibody / podocalyxin

Introduction

Carbohydrate-recognizing antibodies are extremely useful experimental tools for monitoring the changes in cell surface glycan structures as well as for identification of specific glycans on a specific cell type with high sensitivity and strict specificity. This is true in the case of pluripotent stem cells, including human embryonic stem (hES) and human-induced pluripotent stem (hiPS) cells (Wright and Andrews 2009). Among the conventional hiPS/ES cell-marker antibodies, stage-specific embryonic antigen (SSEA)-3 (Shevinsky et al. 1982) and SSEA-4 (Kannagi, Cochran et al. 1983; Kannagi, Levery et al. 1983) specifically recognize globosides such as Gal(β1-3)GalNAc(β1-3)Gal(α1-)-Cer and tumor rejection antigen (TRA)-1-60 (Andrews et al. 1984), TRA-1-81 (Andrews et al. 1984), germ cell tumor monoclonal (GCTM)2 (Pera et al. 1988; Cooper et al. 1992) and GCTM343 (Pera et al. 1988) recognize keratan sulfate (Adewumi et al. 2007). Keratan sulfate is a class of glycosaminoglycan (GAG). But in contrast to other GAGs, it does not contain uronic acids, and its repeating disaccharide unit is composed of alternating D-galactose (Gal) and *N*-acetyl-D-glucosamine (GlcNAc) residues. In most cases, the hydroxyl groups at the C-6 position of GlcNAc residues and/or Gal residues are sulfated. The keratan sulfate-glycan chains are linked to the polypeptide backbone through either *N*- or *O*-linkages, and are occasionally modified with sialic acid and fucose.

It should be kept in mind, however, that most of the above antibodies were generated against hEC cells: 2102Ep for

[1]To whom correspondence should be addressed: Tel: +81-77-3444; Fax: +81-77-3496; e-mail: tkawasak@fc.ritsumei.ac.jp
[†]A JSPS research fellow.

TRA-1-60, TRA-1-81 and SSEA-4 and GCT27 for GCTM2 and GCTM343. In other words, these antibodies are not specific to hiPS/ES cells; rather, they recognize those glycans that are common to hiPS/ES and embryonal carcinoma (EC) cells. ES cells and EC cells are very closely related cells and have many properties in common, but EC cells are teratocarcinoma. New antibodies that are capable of distinguishing between malignant and normal phenotype would be valuable. With this background, we tried to generate antibodies specific to hiPS cells. We first selected hiPS cell-positive hybridomas, from which hEC cell-positive hybridomas were excluded. By this procedure, we have obtained three antibodies that are capable of distinguishing between hiPS/ES and hEC cells. From these novel antibodies, we have chosen one, designated R-10G, and the biochemical properties of the antibody and its epitope molecules have been investigated. The results demonstrated clearly that R-10G is a novel marker antibody recognizing a type of keratan sulfate lacking oversulfated structures on hiPS cells, and thus should be useful not only as a new molecular probe for disclosing the roles of glycans on the surface of hiPS cells in the maintenance of self-renewal and pluripotency and during the process of differentiation, but also as a potent tool for the evaluation and standardization of hiPS cells with different tissue origins and different histories in regenerative medicine.

Results

Generation of monoclonal antibodies to hiPS cells

In order to raise a panel of monoclonal antibodies to cell surface markers on hiPS cells, freeze-thawed Tic cells in phosphate-buffered saline (PBS) were mixed with Freund's complete adjuvant (FCA) and used to immunize C57BL/6 mice intraperitoneally or subcutaneously. Primary screening of a total of 960 hybridomas using Tic cell-fixed plates and MRC-5 cell-fixed plates (controls) indicated that 29 hybridomas produced antibodies that exhibited reactivity to surface antigens on Tic cells. Secondary screening was performed for these hybridomas to determine the reactivities of the antibodies to a hEC cell line, 2102Ep and mouse embryonic fibroblast (MEF).

Table I. Summary of hybridoma screening by cell plate binding assaying

No.	Tic	2102Ep	MRC-5	MEF	No.	Tic	2102Ep	MRC-5	MEF
1	++	+++	±	−	16	+	+	±	±
2	+++	++	+	−	17	++++	±	−	−
3	+	+	−	−	18	++	++	−	−
4	+++	++	−	−	19	+++	+++	−	−
5	++	±	−	−	20	+++	+++	++	±
6	+++	+++	+	−	21	+++	+++	+	±
7	++	++	±	−	22	++	++	−	−
8	+	+++	+	−	23	++	++	++	−
9	+++	+++	−	−	24	+	+	−	−
10	+++	±	−	−	25	++	+++	+	±
11	+++	+	−	−	26	++++	+++	−	−
12	+	++++	−	−	27	+++	+++	+	−
13	+++	+++	±	±	28	+++	+++	−	−
14	++	+	−	−	29	+++	+++	−	−
15	+	++	−	−					

The culture supernatant of each hybridoma was added to cell-fixed screening plates (Tic, 2102Ep, MRC-5 and MEF cells), and binding of antibodies to the cells was monitored by DAB staining under a light microscope after treatment with HRP-conjugated anti-mouse IgG as described under Materials and methods. The results are presented as a 5-grade scale from − to ++++.

As shown in Table I, a large portion of the antibody panel (Nos. 2, 4, 6, 9, 13, 19, 20, 21, 25, 26, 27, 28 and 29) exhibited significant binding activity not only to Tic cells but also to 2102Ep cells, an EC cell line. Interestingly, however, antibody Nos. 10, 11 and 17 exhibited strong reactivity toward Tic cells but no or very weak reactivity toward 2102Ep cells. These results demonstrated clearly that there are definite differences in the antigen profiles between hiPS and hEC cells, even though there is considerable overlapping between them. The binding of these antibodies to human iPS cells was confirmed by western blotting, in which Tic cell lysates were resolved by sodium dodecyl sulfate–polyacrylamide gel electrophoresis (SDS–PAGE) and the culture supernatants of hybridomas were used as primary antibodies. The protein profiles of SDS–PAGE and some representative western blot profiles of Tic cell lysates (7/29 hybridomas) are presented in Figure 1A and B, respectively.

Tic cell lysates gave a large number of protein bands corresponding to from 15 to >300 kDa. On the other hand, the migration positions and the intensities of the immunoreactive bands were characteristic of the respective hybridomas, but these bands appear to be classifiable into three groups on the basis of their apparent molecular sizes: Between 35 and 50 kDa (e.g. clone 27), between 75 and 100 kDa (e.g. clone 25) and over 250 kDa (e.g. clones 10 and 26). Such antibodies that show strong binding in the cell plate assay but a faint or essentially no band on western blotting might interact with

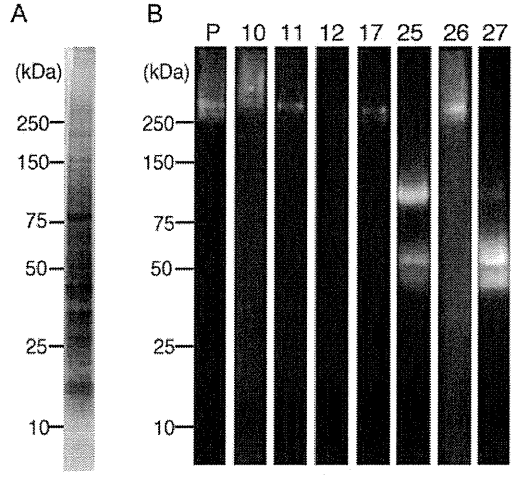

Fig. 1. Screening of hybridomas by western blotting. Tic cell lysates in the complete RIPA buffer (15 μg protein) were resolved by SDS–PAGE on a 4–15% gradient gel under nonreducing conditions, followed by immunoblot detection with antibodies secreted into the medium from the respective hybridomas as described under Materials and methods. (**A**) Gel code blue staining of SDS–PAGE of the Tic cell lysates. (**B**) Western blotting. The numbers at the top of each column indicate the clone number of hybridomas. P: Antibody TRA-1-60 (positive control). The molecular mass markers are shown on the left.

membrane lipid components (e.g. clones 11, 12 and 17). In lane P, TRA-1-60, a conventional iPS/ES marker antibody, which was used as a positive control, gave a single but a diffuse band in the high-molecular-weight region over 250 kDa, as was expected from a previous report (Andrews et al. 1984). The results of the cell-binding assay indicated that three hybridomas Nos. 10, 11 and 17 seemed to be appropriate to pursue our aim. Of these hybridomas, we focused on No. 10, since these hybridomas exhibited a most striking band upon western blotting as shown in Figure 1B. The hybridoma R-10G was a subclone obtained from hybridoma No. 10. The isotype of antibody R-10G is IgG1.

Binding properties of R-10G as to iPS/ES/EC cells

We examined the binding activity of R-10G toward some other hiPS/ES/EC cell lines using an InCell analyzer 2000 in comparison with those of conventional hiPS and mouse iPS/ES marker antibodies, TRA-1-81, TRA-1-60, SSEA-1, SSEA-3 and SSEA-4. The results of immunocytochemical studies are summarized in Figure 2 (A–F). As shown in (A), antibody R-10G interacted remarkably with three different hiPS cell lines: Tic cells (68 ± 7%, mean percentage binding in four experiments ± SD), 201B7 cells (88 ± 7%) and Squeaky cells (79 ± 9%), and also with two hES cell lines: H9 cells (64 ± 4%) and KhES-3 cells (83 ± 2%). TRA-1-81 (B), TRA-1-60 (C), SSEA-3 (D) and SSEA-4 (E) also exhibited high binding activities of 96–99, 94–99, 64–72 and 85–99%, toward these five types of hiPS/ES cells, respectively, all being consistent with previous studies (Wright and Andrews 2009). These results indicated that R-10G is a hiPS/ES-recognizing antibody like the other conventionally used hiPS/ES marker antibodies. Most importantly, however, in contrast to the other conventional iPS/ES marker antibodies, which bound to an EC cell line, 2102Ep, as effectively as to other iPS/ES cells (68–98%), R-10G did not bind to an EC cell line, 2102Ep, significantly (6 ± 1%) (A). This was confirmed by essentially no binding of R-10G to a different EC cell line, NCR-G3 (data not shown). Taken together, these results indicated clearly that R-10G is a unique iPS/ES marker antibody, which distinguishes between hiPS and hEC cells. SSEA-1 (in F), which is known to be negative as to undifferentiated hiPS/ES/EC cells (Wright and Andrews 2009) did not show significant binding to any of the cell lines used in this experiment, as expected.

Then, we examined the localization of these epitopes on the surface of hiPS (Tic) cells by means of immunocytochemical experiments using a laser confocal scanning microscope. As shown in Figure 3 (A and B), at a low magnification (×100), almost all the TO-PRO 3 (nuclear counterstained)-positive cells in a colony appeared to be stained with R-10G in green, although there were significant differences at the level of staining depending upon the cells. TRA-1-81 appeared to stain also almost all cells ubiquitously in red. However, when the two images were merged into a single one, it was found that the cells in the central region of the colony were largely stained in green, while those in the peripheral region were largely stained in red. This apparent polarity of the epitope expression may be

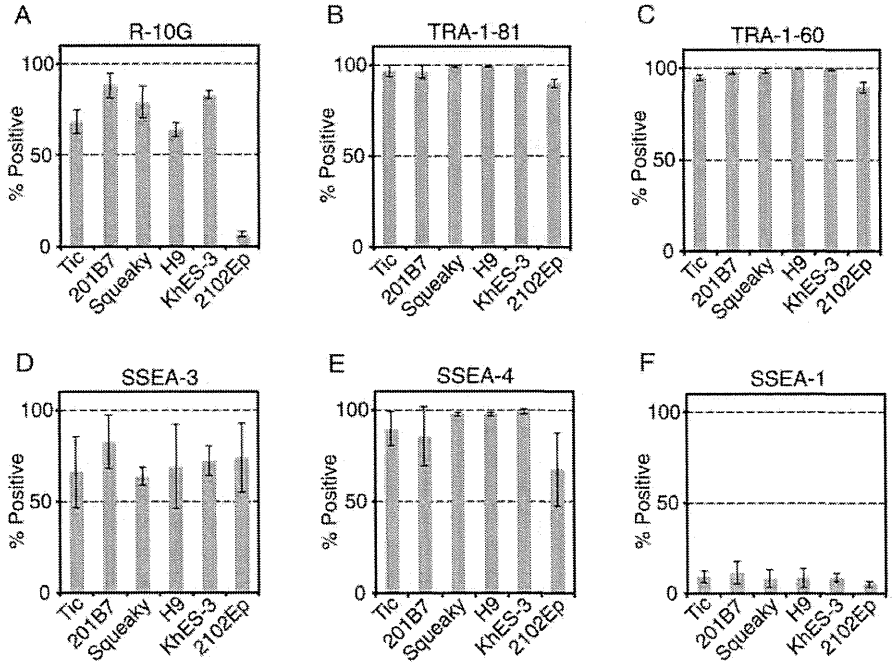

Fig. 2. Characterization of R-10G as an iPS/ES marker antibody using an InCell Analyzer. HiPS cells (Tic, 201B7, and Squeaky), hES cells (H9 and KhES-3) and hEC cells (2102Ep) seeded onto 24-well plates were fixed in 4% PFA and then incubated with monoclonal antibodies (R-10G, TRA-1-81, TRA-1-60, SSEA-3, SSEA-4 and SSEA-1) at 4°C overnight. Binding of antibodies to the cells was visualized by incubation with Alexa Fluor 647-conjugated chicken anti-mouse IgG and then quantitated using an InCell Analyzer 2000 and Developer Toolbox ver1.8 as described under Materials and methods. Error bars represent standard deviation from the mean ($n = 4$).

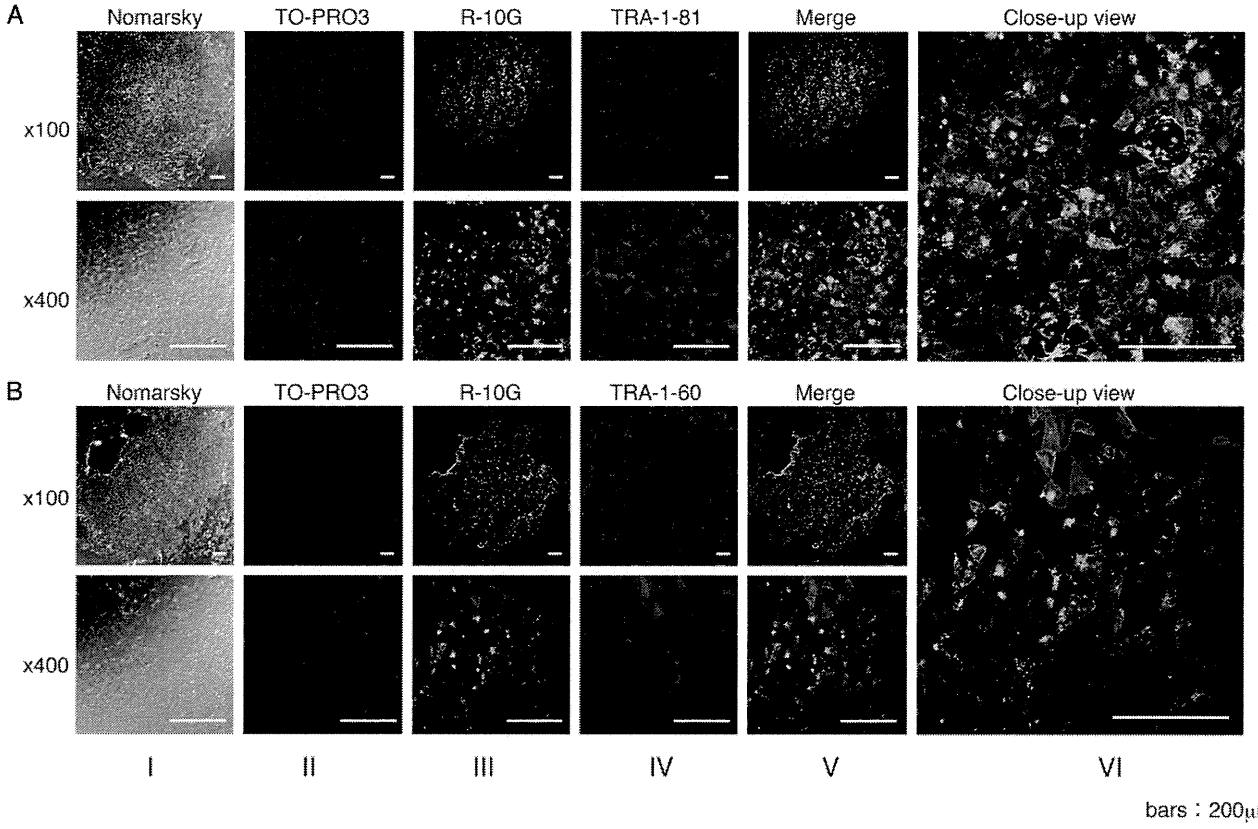

Fig. 3. Localization of the R-10G, TRA-1-81 and TRA-1-60 epitopes on cultured Tic cells visualized on laser confocal microscopy. (**A**) Tic cells cultured on Millipore EZ slides were double-stained first with R-10G and Alexa Fluor 488-conjugated secondary (anti-mouse IgG1) antibody, followed by with TRA-1-81 and Alexa Fluor 555-conjugated secondary (anti-mouse IgM) antibody. Cells were observed at two different magnifications: ×100 (upper panel) and ×400 (lower panel). (I) Nomarski imaging. (II) Nuclear counterstaining with TO-PRO3. (III) Antigens for R-10G (green). (IV) Antigens for TRA-1-81 (red). (V) Merged image of (III) and (IV). (VI) Close-up view of V (×400). (**B**) Cultured Tic cells were double-stained first with R-10G and Alexa Fluor 488-conjugated secondary antibodies, followed by with TRA-1-60 and Alexa Fluor 555-conjugated secondary antibodies, and visualized as described in (**A**). (I)–(IV) are the same as in (**A**) except for (IV), in which antigens for TRA-1-60 are shown in red. Scale bars, 200 μm.

related to some micro-environmental differences between the central and peripheral regions of a hiPS colony. At a higher magnification (×400, in A and B), the R-10G staining was detected on the surface and boundaries of the cells, but at the same time granular structures stained strongly in green were found in the cytosol. These granular structures were hardly seen in TRA-1-81 and TRA-1-60 stained images, and the red staining was predominantly detected on the surface of the cells. In merged images, some Tic cells were stained in green and the other cells in red, although there were cells or subcellular regions of cells that were stained in yellow, suggesting that some of the cells expressed predominantly either the R-10G or TRA-1-81 epitope, or either the R-10G or TRA-1-60 epitope. However, there were a significant number of cells that co-expressed these two pairs of epitopes (R-10G and TRA-1-81 epitopes and R-10G and TRA-1-60 epitopes) in comparable ratios in close vicinity. These results suggested that hiPS cells are in fact heterogeneous with regard to the expression of cell surface glycans from cell to cell, and suggested the presence of subtypes of cells within a single colony of hiPS cells.

Identification of the R-10G antigen molecule as a podocalyxin

On the basis of the results of western blotting of Tic cell lysates with clone 10 (Figure 1B), which gave a single but diffuse high-molecular-weight protein band, we tried to isolate the presumptive antigen molecule by using an affinity column of R-10G. Freeze-thawed hiPS cells were solubilized in the complete RIPA buffer (see Materials and methods), and the lysate was applied to an R-10G-Sepharose 4B column. Proteins bound to the column and eluted with pH 11.5 buffer were analyzed by western blotting. As shown in Figure 4A, column 1, a single but diffuse R-10G positive band was observed at the same position as that in the case of the whole cell lysate (Figure 1B, clone 10). The isolated antigen was subjected to SDS–PAGE and the resolved protein bands were stained with SYPRO Ruby Protein Gel Stain. The bands corresponding to those on western blotting were excised as three fractions (a, b and c in column 2), and then subjected to *in-gel* trypsin digestion, and the peptides released were analyzed by LC/MS/MS. The three fractions of the major western blotting band generated several peptides sequences, all of which

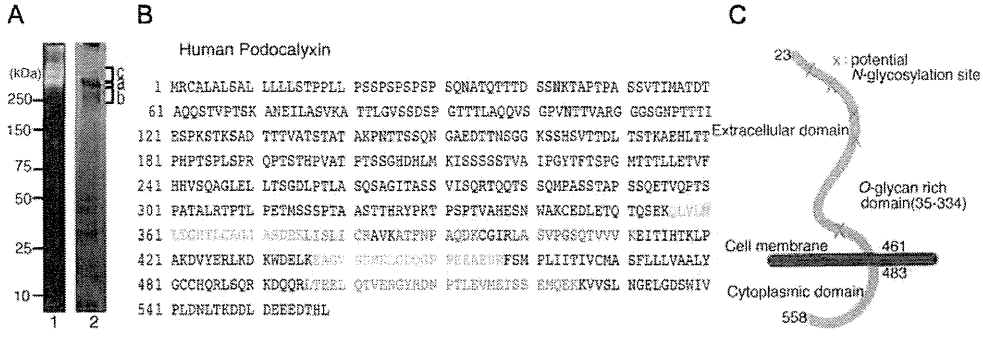

Fig. 4. Isolation and identification of the antigen protein carrying the R-10G epitope. (**A**) R-10G antigen proteins isolated from Tic cell lysates with an R-10G-affinity column were resolved by SDS–PAGE on a 4–15% gradient gel under nonreducing conditions. The resolved proteins were transferred to a PVDF membrane, followed by immunoblot detection with R-10G (column 1, the isolated antigens derived from 5×10^4 cells). The molecular mass markers are shown on the left. The gel was stained with SYPRO Ruby Protein Gel Stain (column 2, the isolated antigens derived from 3.5×10^5 cells), and the protein bands, a, b and c, i.e. the middle/major, higher and lower molecular size immunoblot bands, were excised from the gel. After *in-gel* trypsin digestion, the peptides released from the gel were subjected to LC/MS/MS analysis as described under Materials and methods. (**B**) Identification of the R-10G antigen protein by MS. The identified peptides in bands a, b and c are shown in red letters, those in bands a and b in blue and those in band b in green within the complete human podocalyxin sequence. The potential *N*-glycosylation sites (33, 43, 104, 144 and 360) are indicated by yellow-shaded areas. (**C**) Schematic representation of the membrane topology of human podocalyxin.

corresponded to partial sequences of human podocalyxin (Figure 4B), and no other alternative sequence was detected for these fractions *a*, *b* and *c*.

Podocalyxin is a heavily glycosylated type-1 transmembrane protein belonging to the CD34 family of sialomucins (Sassetti et al. 1998, 2000) (Figure 4C). The protein was originally described as the major sialoprotein on podocytes of the kidney glomerulus (Kerjaschki et al. 1984). Recently, podocalyxin was shown to be expressed by hematopoietic progenitors, vascular endothelia and a subset of neurons, and it is aberrantly expressed in a number of tumors (Nielsen and McNagny 2009). The human podocalyxin gene (Kershaw, Wiggins et al. 1997) encodes a protein of 558 amino acids. Because the extracellular domain of podocalyxin is extensively glycosylated with sialylated *O*-linked carbohydrates and five potential *N*-linked glycosylation sites, the approximate molecular weight of podocalyxin is 160–165 kDa (Kershaw, Beck et al. 1997). Interestingly, podocalyxin was identified to be highly expressed in undifferentiated hES cells (Brandenberger et al. 2004; Cai et al. 2006). In addition, the TRA-1-81 and TRA-1-60 epitopes have been shown to be expressed on a 200 kDa form of podocalyxin (Schopperle and DeWolf 2007). Identification of podocalyxin as the R-10G antigen protein constituted evidence that podocalyxin polypeptide serves as a common carrier for a family of epitopes generated through carbohydrate modifications on the human pluripotent cell surface.

Characterization of the R-10G epitope by glycosidase digestion and western blotting

The unusual diffuse shape of the R-10G reactive band (Figure 1B, clone 10 and Figure 4A) suggested that the band is most probably of a glycoprotein. To examine this, we digested a Tic cell lysate and/or R-10G antigen isolated therefrom with various glycosidases prior to SDS–PAGE, and determined the effects of these treatments on the intensities and the migration positions of the R-10G reactive bands. This experiment was carried out with two other hiPS/ES marker antibodies, TRA-1-81 and TRA-1-60, which have been shown to recognize keratan sulfate (Adewumi et al. 2007) and sialylated keratan sulfate (Badcock et al. 1999), respectively.

As shown in Figure 5A (lanes 1, 3 and 5), upon western blotting, Tic cell lysates gave diffuse bands not only with R-10G but also with TRA-1-81 and TRA-1-60 in high-molecular-weight regions (>250 kDa), this being consistent with the potent immunocytochemical activities of these antibodies toward Tic cells, as described above. Then, we examined the reactivity of the isolated R-10G antigen toward R-10G, TRA-1-81 and TRA-1-60 (Figure 5A, lanes 2, 4 and 6). Unexpectedly, the isolated R-10G antigen reacted not only with R-10G but also with TRA-1-81 and TRA-1-60, giving a single band at the respective positions expected from those for the Tic cell lysates. These results suggested that these three antibodies recognize similar glycans in the same category, keratan sulfate, as their epitopes. In agreement with this hypothesis, upon digestion of the R-10G antigen with keratanase II, which degrades keratan sulfate specifically (see Figure 6), the R-10G epitope as well as the TRA-1-81 epitope was degraded (Figure 5B). It should be noted, however, that the most of the R-10G epitope disappeared easily with a small amount of the enzyme, whereas the TRA-1-81 epitope was relatively stable as to the digestion and was degraded only when a large amount of the enzyme was added. These results suggested that R-10G and TRA-1-81 share a common epitope, keratan sulfate, although the epitope structures recognized by these antibodies are different from each other in some unspecified way.

Following this initial experiment involving keratanase II, we studied the properties of the R-10G epitope by the same means with various GAG-degrading enzymes. As shown in Figure 5C, chondroitinase ABC, which degrades essentially all the chondroitin sulfate subfamily, and the heparinase mix, a mixture of heparinase, heparitinase I and heparitinase II,

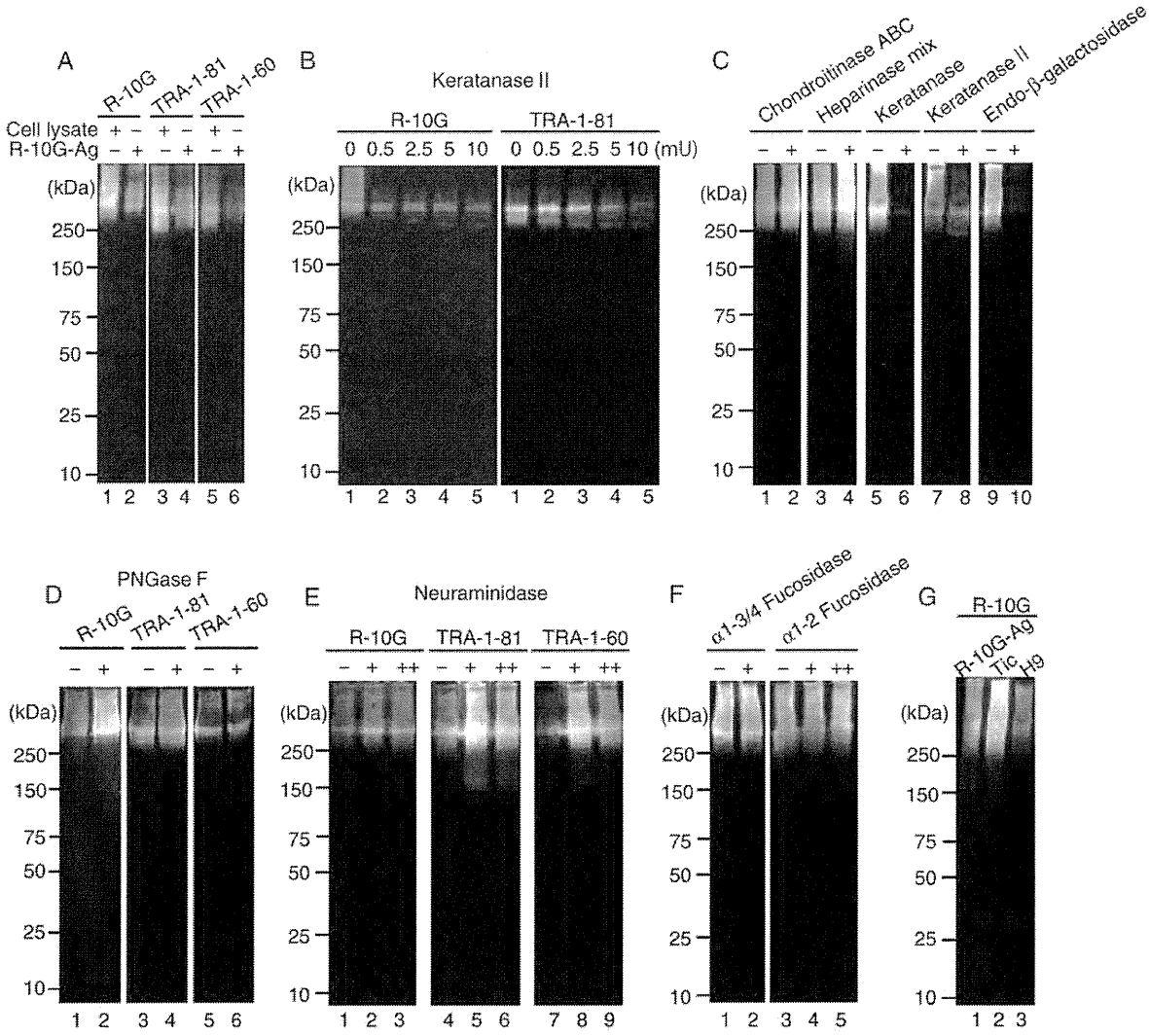

Fig. 5. Characterization of the R-10G epitope by glycosidase digestion and western blotting. Tic cell lysates (12 μg protein, corresponding to 1×10^5 cells) and/or the isolated R-10G antigen (corresponding to $\sim 1 \times 10^5$ cells), which had been incubated with and without predigestions with various glycosidases, were subjected to SDS–PAGE on a 4–15% gradient SDS-polyacrylamide gel under nonreducing conditions except for PNGase F digestion, followed by western blotting with R-10G and other undifferentiated cell-marker antibodies as described under Materials and methods. (**A**) Western blotting of Tic cell lysates and the R-10G antigen with R-10G, TRA-1-81 and TRA-1-60. (**B**) The R-10G antigen was digested with increasing amounts of keratanase II and the digests were analyzed by western blotting with R-10G and TRA-1-81. (**C**) The R-10G antigen was digested with chondroitinase ABC (lane 2), heparinase mix (lane 4), keratanase (lane 6), keratanase II (lane 8) or endo-β-galactosidase (lane 10) and the digests were analyzed by western blotting with R-10G. Lanes 1, 3, 5, 7 and 9: No enzyme added. (**D**) The R-10G antigen was digested with PNGase F, and the digests were analyzed by western blotting with R-10G (lane 2), TRA-1-81 (lane 4) and TRA-1-60 (lane 6). Lanes 1, 3 and 5: No enzyme added. (**E**) The R-10G antigen was digested with neuraminidase from *Arthrobacter ureafaciens* of 3.75 mU (lanes 2, 5 and 8) or 37.5 mU (lanes 3, 6 and 9) and the digests were analyzed by western blotting with R-10G (lanes 1, 2 and 3), TRA-1-81 (lanes 4, 5 and 6) and TRA-1-60 (lanes 7, 8 and 9). Lanes 1, 4 and 7: No enzyme added. (**F**) The R-10G antigen was digested with α1–3/4 fucosidase (lane 2: 15 μU) or α1–2 fucosidase (lanes 4 and 5: 0.33 and 2.0 U, respectively), and the digests were analyzed by western blotting with R-10G. Lanes 1 and 3: No enzyme added. (**G**) The R-10G antigens (lane 1), Tic cell lysates (15 μg protein, lane 2) and H9 cell lysates (15 μg protein, lane 3) were analyzed by western blotting with R-10G. The molecular mass markers are shown on the left of the respective panels, **A**–**G**.

which degrades various subtypes of heparan sulfates and heparins, did not decrease the R-10G binding activity; rather, the reactivity was enhanced to some extent for some undetermined reasons. These results indicated that neither heparan sulfate/heparin nor chondroitin sulfates are associated with the epitope structure as major constituents. On the other hand, keratanase and endo-β-galactosidase, both of which are keratan sulfate-degrading enzymes, abolished the R-10G binding activity as keratanase II did, confirming that the major epitope of R-10G is a keratan sulfate (see Figure 6).

Then, we studied the effect of PNGase F treatment. As shown in Figure 5D, PNGase F digestion of the R-10G antigen resulted in no decrease in the R-10G binding activity or the migration position of the major reactive band,

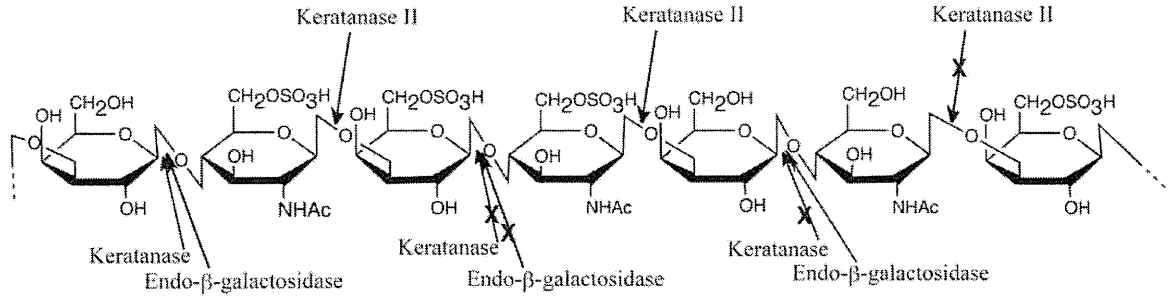

Fig. 6. Structural requirements of keratan sulfate-degrading enzymes. Schematic presentation of the specificities of keratanase II, keratanase and endo-β-galactosidase with regard to the effect of sulfate modification of the structural repeating units of keratan sulfate. The arrows marked with X indicate that the enzyme does not work.

indicating that *N*-linked glycans are not the major constituents of the epitope on the antigen. The same results were obtained for TRA-1-81 and TRA-1-60, excluding the major role of *N*-glycans as the epitope constituents.

The isolated R-10G antigen contained significant amounts of sialic acid and fucose (see Discussion). Since it was reported previously that the TRA-1-60 epitope was sialylated keratan sulfate, which was destroyed on digestion with neuraminidase either from *Vibrio cholerae* or from *Arthrobacter ureafaciens* (Andrews et al. 1991; Badcock et al. 1999). We examined the effects of these two neuraminidases on the immunoreactivity of the R-10G antigen by western blotting. As shown in Figure 5E, digestion of the R-10G antigen with neuraminidase from *Arthrobacter ureafaciens* resulted in no significant change in the immunoreactive bands for R-10G (lanes 1–3). The same results were obtained for the R-10G antigen with neuraminidase from *Vibrio cholerae* (data not shown). These results indicated that sialic acids are not associated with the R-10G epitope as a major constituent. Similarly, the reactivities of TRA-1-81 and TRA-1-60 to the R-10G antigen were not diminished upon digestion with neuraminidase from *Arthrobacter ureafaciens* (lanes 4–9). Instead, their reactivities were enhanced (lane 4 vs. lanes 5, 6, lane 7 vs. lanes 8, 9), suggesting that sialylation blocks or sterically hinders these epitopes. The same results were obtained with neuraminidase from *Vibrio cholerae* (data not shown).

Recently, the Fuc(α1-2)Gal(β1-3)GlcNAc structure has been reported to be a pluripotency-associated epitope for SSEA-5, a newly established hES marker monoclonal antibody (Tang et al. 2011), and for BC2LCN, a lectin isolated from a Gram-negative bacterium *Burkholderia cenocepacia* (Sulak et al. 2010; Tateno et al. 2011). Then, we studied the effects of α-fucosidase treatment on the immunoreactivity of the R-10G antigen. As shown in Figure 5F, digestion of the R-10G antigen neither with α1-3/4 fucosidase nor with α1-2 fucosidase indicated any detectable changes on the immunoreactive bands, excluding the major roles of fucose residue as the R-10G epitope constituents and exhibiting the differences in binding specificity between R-10G and SSEA-5 or BC2LCN.

Figure 5G demonstrated that the R-10G epitope was expressed also on hES cells. Upon western blotting, an H9 cell extract, prepared by the same procedure as described above for Tic (hiPS) cells under Materials and methods, gave an R-10G positive band almost at the same position as for the iPS (Tic) cell lysates and also for the R-10G antigen isolated therefrom. These results are consistent with those of image analysis (Figure 2), in which R-10G bound to two hES cell lines, H9 and KhES-3, as effectively as to iPS cell lines, Tic, 2101B7 and Squeaky, like most of the conventional hiPS/ES marker antibodies.

Further characterization of the R-10G epitope by chemical analysis

In the next experiment, the oligosaccharides released from the R-10G antigen with keratan sulfate-degrading enzymes were analyzed by reverse-phase ion-pair HPLC system using a fluorometric post-column detection method newly developed by Hirose et al (in preparation). Figure 7A shows the oligosaccharide profiles released with keratanase II, which hydrolyzes the 1,3-β-glucosaminidic linkages to galactose in keratan sulfate, when the 6-O-position of GalNAc is sulfated (Brown et al. 1995; Oguma et al. 2001) (see Figure 6). A predominant peak was detected at 6.60 min, which corresponds to the disaccharide-repeating units of keratan sulfate, Gal-GlcNAc (6S) (peak 1), followed by a small peak corresponds to Gal-GlcNAc(6S)-Gal-GlcNAc(6S) (peak 2) and some very minor peaks, which include a negligible peak at the position corresponded to Gal(6S)-GlcNAc(6S) (peak 3). The sulfation index of the GAG family, the average number of sulfate residues per disaccharide-repeating unit, Gal-GlcNAc, was calculated to be 1.02. Figure 7B shows the oligosaccharide profiles released with endo-β-galactosidase, which hydrolyzes the 1,4-β-galactosidic linkage when the 6-O-position of the Gal residue is not sulfated, irrespective of the presence or absence of sulfate on the adjacent GalNAc (Fukuda and Matsumura 1976). One major peak was detected at 6.36 min, which corresponds to the disaccharide-repeating units of keratan sulfate, GlcNAc(6S)-Gal (peak 5), followed by several significant peaks between peak 5 and peak 6. Figure 7C shows the elution profile of endo-β-galactosidase digests of the keratan sulfate from bovine cornea, which was used as a standard of keratan sulfate. Three major peaks such as peaks 5, 6 and 7 were obtained, which correspond to GlcNAc(6S)-Gal, GlcNAc (6S)-Gal(6S)-GlcNAc(6S)-Gal and GlcNAc(6S)-Gal (6S)-GlcNAc(6S)-Gal(6S)-GlcNAc(6S)-Gal, respectively. The presence of peaks 6 and 7 in Figure 7C but no or little peaks at the corresponding positions in Figure 7B may be explained by

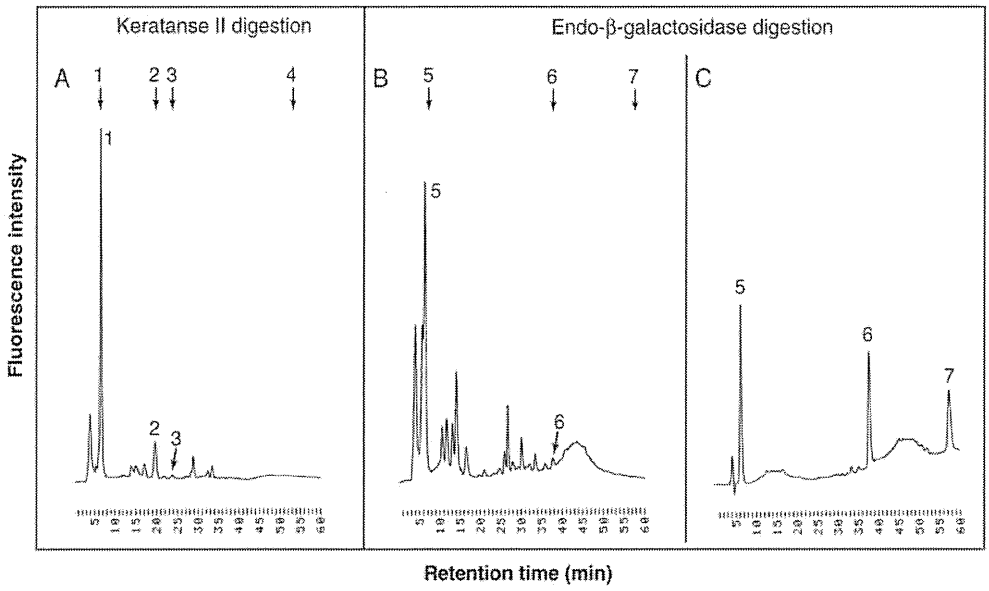

Fig. 7. HPLC profiles of keratan sulfate-derived oligosaccharides. (**A**) The R-10G antigen was digested with keratanase II and the digests were submitted to HPLC as described under Materials and methods. (**B**) The R-10G antigen was digested with endo-β-galactosidase and the digests were submitted to HPLC as in (**A**). (**C**) A standard keratan sulfate from bovine cornea was digested with endo-β-galactosidase and the digests were submitted to HPLC as in (A). Arrows: 1, Gal-GlcNAc(6S); 2, Gal-GlcNAc(6S)-Gal-GlcNAc(6S); 3, Gal(6S)-GlcNAc(6S); 4, Gal(6S)-GlcNAc(6S)-Gal(6S)-GlcNAc(6S); 5, GlcNAc(6S)-Gal; 6, GlcNAc (6S)-Gal(6S)-GlcNAc(6S)-Gal; 7, GlcNAc(6S)-Gal(6S)-GlcNAc(6S)-Gal(6S)-GlcNAc(6S)-Gal.

a considerable level of oversulfated structure (sulfation at C-6 of Gal residues) in the keratan sulfate from bovine cornea and in contrast by a negligible level of this sulfation in the R-10G epitope. This is in accordance with a substantially higher sulfation index of the keratan sulfate from bovine cornea, 1.29, than that of the R-10G antigen, 1.02, as described above. It is possible that several significant peaks between peak 5 and peak 6 in Figure 7B may represent additional modifications such as fucosylation, sialylation or something else of Gal residues in the keratan sulfate in the R-10G antigen.

Taking all these results into account, it is reasonable to conclude that the R-10G epitope is a unique keratan sulfate lacking oversulfated structures.

Characterization of R-10G epitopes by ELISA

In this experiment, the binding activity of R-10G toward the biotinylated GAG specimens, which had been fixed to the streptavidin-coated plastic wells, was assayed using an enzyme-linked immunosorbent assay (ELISA) system in comparison with that of 5D4, which is known to recognize a high-sulfated keratan sulfate (Mehmet et al. 1986). As shown in Figure 8A, the keratan sulfate from bovine cornea reacted effectively with R-10G, while the other GAGs, hyaluronic acid, chondroitin, chondroitin sulfate from whale cartilage, chondroitin sulfate from the spinal column of *Acipenser mediros-tris*, chondroitin sulfate B, chondroitin sulfate C, chondroitin sulfate D, chondroitin sulfate E and heparan sulfate, did not show any significant binding activity toward R-10G, indicating clearly that the binding specificity of R-10G is very strict for keratan sulfate. In this respect, R-10G is similar to 5D4 (Figure 8B). It should be noted, however, that there is >100-fold difference in the amount of antibodies required to generate adequate responses between these two antibodies, 0.008 μg/mL for 5D4 and 1 μg/mL for R-10G. This may indicate that the keratan sulfate from bovine cornea is abundant in the 5D4 epitope but is scarce in the R-10G epitope. A marked difference between R-10G and 5D4 was also demonstrated by inhibition studies.

As shown in Figure 8C, the binding of R-10G to the keratan sulfate from bovine cornea in the plastic plates was inhibited by the same keratan sulfate in proportion to the amount of the keratan sulfate added to the incubation mixture, as expected. In contrast, a high-sulfated keratan sulfate (KSP-1), which was isolated from shark cartilage according to the procedure as described by Furuhashi (Furuhashi 1961), did not inhibit the R-10G binding at all, indicating the inability of R-10G to bind to a high-sulfated keratan sulfate. On the other hand, as shown in Figure 8D, a highly sulfated-keratan sulfate (KSP-1) inhibited the 5D4 binding approximately 100 times more than that of the keratan sulfate from bovine cornea, confirming the highly specific binding of 5D4 to a high-sulfated keratan sulfate (Mehmet et al. 1986).

In the next experiment, when the keratan sulfate fixed on a well was digested with keratanase II, the R-10G binding activity disappeared almost completely (Figure 8E), as the 5D4 binding activity did (Figure 8F). When the keratan sulfate was digested with keratanase, the R-10G binding activity disappeared again almost completely (Figure 8E), while the 5D4 binding activity was reduced only partially (~40%) (Figure 8F). This differential susceptibility to keratanase between the R-10G and 5D4 epitopes is most probably due to the substrate specificity of keratanase, which digests the keratan sulfate only when C-6 of the GalNAc is sulfated but C-6 of the galactose residue is not sulfated (Ito et al. 1986)

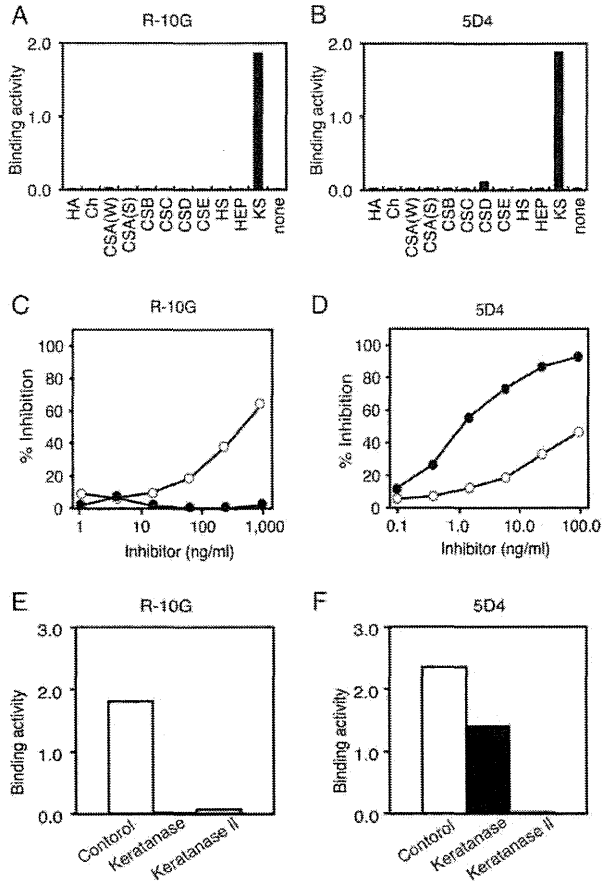

Fig. 8. Characterization of the R-10G epitope by ELISA. (**A**) Binding activities of R-10G toward various GAGs were determined. GAGs used: HA (hyaluronic acid), Ch (chondroitin from shark cartilage), CSA (W) (chondroitin sulfate from whale cartilage), CSA (S) (chondroitin sulfate from the spinal column of *Acipenser medirostris*), CSB (chondroitin sulfate B), CSC (chondroitin sulfate C), CSD (chondroitin sulfate D), CSE (chondroitin sulfate E), HS (heparan sulfate) and KS (keratan sulfate). IgG1 from murine myeloma was added to the GAG-coated plates and the amounts of IgG1 bound to the plates were determined as negative controls. (**B**) Binding activities of 5D4 toward various glycosaminoglycans were determined as described in (**A**). (**C** and **D**) Inhibitory effects of two keratan sulfates from different origins on the antibody binding to keratan sulfate from bovine cornea. To assay mixtures containing R-10G (**C**) or 5D4 (**D**), increasing amounts of KS (keratan sulfate from bovine cornea) (open circle) or KPS-1 (high-sulfated keratan sulfate form shark cartilage) (filled circle) were added, and the effects of these inhibitors on the binding activity were determined as described in (**A**). (**E** and **F**) Different sensitivities of the R-10G and 5D4 epitope structures to keratan sulfate-degrading enzymes. Biotinylated keratan sulfate from bovine cornea, which had been treated with either no enzyme (white bars), keratanase (black bars), or keratanase II (dashed bars) at 37°C overnight, was fixed on a streptavidin-coated plate (1 μg/mL), and the binding activity of R-10G (1 μg/mL) (**E**) or 5D4 (0.008 μg/mL) (**F**) to the residual oligosaccharide moieties on the plates were assayed as described in (**A**).

(see Figure 6). The 5D4 epitope is a high-sulfated keratan sulfate, and C-6 of the galactose linked to GalNAc is frequently sulfated and resistant to keratanase digestion. Conversely, these results suggested that C-6 of the galactose residues in the R-10G epitope is mostly not sulfated.

Finally, these studies involving an exogenous keratan sulfate and 5D4 antibodies confirmed strongly the conclusions made with the endogenous antigen molecule on hiPS cells and R-10G, as described above.

Tissue distribution of the R-10G epitope

Conventional hiPS/ES/EC marker antibodies are expressed not exclusively on hiPS/ES/EC cells but the same or cross-reactive epitopes are occasionally expressed either in fetal or adult tissues. For example, TRA-1-81 reacted with human mammary ducts, stomach, the small and large intestine and others, and TRA-1-60 reacted with human smooth muscle cells, the intestine, lung, skin, uterus and others, in addition to hEC cells (Andrews et al. 1984). In this connection, we examined the tissue distribution of the R-10G epitope by immunohistochemistry studies of human adult and fetal tissues using a human tissue array. Out of 32 human adult and fetal tissues tested, adult brain and adult cerebellum showed strong reactivity to R-10G, which are comparable to that for Tic cells. In contrast, the other adult and fetal tissues, that is, placenta, bladder, brain (fetal), cerebellum (fetal), colon, heart, kidney, liver, lung, skin, skeletal muscle, small intestine, spleen, stomach, thymus and tongue did not show any significant staining to the R-10G except for the fetal liver, in which weak spots like islets were detected. Thus, the molecules recognized by R-10G are not confined to hiPS/ES cells but they are expressed on a very limited number of tissues in a unique fashion. In agreement with this staining profile of human tissues, the keratan sulfate isolated from the mouse brain and the rat brain were shown to have sulfation indexes of 1.04 and 1.08, respectively (Oguma et al. 2001), which are close to that of the R-10G antigen on hiPS cells, 1.02.

Discussion

We have established a monoclonal antibody, R-10G, which is a unique iPS/ES marker antibody distinguishing hiPS cells (normal cells) and hEC cells (teratoma cells). Using an affinity column of the R-10G antibody, the R-10G antigen molecule was isolated from hiPS cells and subjected to characterization from various aspects.

The initial characterization of the glycan epitope of R-10G on the hiPS cell surface was carried out with western blotting by comparing the R-10G antigen profiles before and after glycosidase digestion. Of the various glycosidases tested, keratanase II, keratanase and endo-β-galactosidase, all known to degrade keratan sulfate, abolished the R-10G positive band almost completely, indicating that the epitope is a keratan sulfate. However, 5D4, the most widely used keratan sulfate-recognizing monoclonal antibody, did not bind to hiPS cells, as seen on immunocytochemical staining (data not shown). In addition, on western blotting, neither Tic cell lysates nor the R-10G antigen isolated therefrom gave any detectable bands with 5D4 (data not shown). Considering the fact that 5D4 recognizes a high-sulfated keratan sulfate (Mehmet et al. 1986), it was reasonable to assume that the R-10G epitope belongs to a type of keratan sulfate, whose level of oversulfation is low for a keratan sulfate. This assumption was confirmed by ion-pair reverse-phase HPLC

analysis of the digestion products of the R-10G antigen with keratanase II and endo-β-galactosidase. Upon keratanase II digestion, the glycans on the R-10G antigen molecule were shown to be degraded almost completely to the disaccharide-repeating unit of keratan sulfate, Gal-GlcNAc (6S), in parallel with the abolishment of the antibody binding activity, suggesting strongly that the R-10G epitope consists of Gal-GlcNAc(6S) or its tandem repeat structures. This conclusion was confirmed further by the identification of the major component of the endo-β-galactosidase digests as GlcNAc(6S)-Gal. The analysis of the endo-β-galactosidase digests indicated also that there is little sulfation at C-6 of the galactose residues, if any. The sulfation index of the R-10G antigen was calculated to be 1.02. This figure is significantly lower than that of keratan sulfate from bovine cornea, 1.20, and much lower than that of keratan sulfate from bovine cartilage, 1.57 (Oguma et al. 2001). The lack of oversulfation in the R-10 antigen was further confirmed by an ELISA study involving biotinylated keratan sulfate from bovine cornea, which had been fixed on avidin-coated plates as described above.

Taken these results together, it may be reasonable to propose that the R-10G epitope consists of the basic repeating unit of keratan sulfate, Gal-GlcNAc(6S), or its tandem repeat with few oversulfation, which are frequently observed at C-6 of galactose residues in many other keratan sulfates from various origins. However, it is clear that the exact sequence of the R-10G epitope remains to be elucidated and further studies using latest technologies such as glycan sequencing with LC/MS/MS and epitope profiling with carbohydrate microarray platform will be pursued. In this regard, it would be interesting to refer to a recent report (Natunen et al. 2011) that TRA-1-60 and TRA-1-81 require Galβ1-3GlcNAcβ1-3Galβ1-4GlcNAc (a dimeric type 1 lactosamine structure) as a minimum epitope.

Since R-10G, TRA-1-60 and TRA-1-81 share a common carrier protein and the affinity-purified R-10G antigen reacted not only with R-10G but also with TRA-1-60 and TRA-1-81 (Schopperle and DeWolf 2007), the structural relationship between these three immunogenic glycoproteins was speculated. Upon western blotting of the R-10G antigen and Tic cell lysates, slight but significant differences were detected in the migration positions of the respective antibody-reactive bands; they decreased successively in the order of R-10G, TRA-1-60 and TRA-1-81 with some overlapping (see Figure 5A), suggesting that either the size or the number of glycan chains carrying the R-10G epitope may be larger than that of those carrying the TRA-1-60 or the TRA-1-81 epitope. Significant differences were also detected in the relative intensities of the bands of the R-10G antigen as to the corresponding bands of the Tic cell lysates; the ratio decreased from R-10G to TRA-1-60 through TRA-1-81. The R-10G epitope-carrying podocalyxin was most effectively adsorbed to a column, indicating the immunological distinctiveness of these epitopes. The column less effectively captured particularly the TRA-1-60 epitope. The precise glycan structures of these epitopes remain to be elucidated, but the TRA-1-60 and TRA-1-81 epitopes probably belong to a type of keratan sulfate similar to the R-10G epitope, because 5D4, an antibody recognizing a high-sulfated keratan sulfate and BCD4, another commercially available antibody recognizing keratan sulfate, did not bind to hiPS/ES cells (R-10G/TRA-1-60/TRA-1-81 reacting cells) (data not shown), although these epitopes were susceptible to digestions with keratan sulfate-degrading enzymes in vitro (Figure 5B).

Carbohydrate analysis of the R-10G antigen isolated from 1.0×10^6 Tic cells indicated that it contained 370, 84, 1026, 46 and 51 pmol of glucosamine, galactosamine, galactose, sialic acid and fucose, respectively. These figures are consistent with the idea that keratan sulfate is the major glycan constituent of the R-10G antigen. Pronase digestion of the R-10G antigen released glycopeptides, which bound to the R-10G column. Approximately 2/3 of glucosamine applied to the column was recovered in the bound fraction, indicating that the glycan portion of the R-10G antigen plays a crucial role as the epitope and the polypeptide portion of the R-10G antigen may not be associated with the epitope activity. Since some of the hiPS/ES marker epitopes such as SSEA-3 and SSEA-4 are expressed on glycolipids, we examined whether or not the R-10G epitope is expressed on glycolipids as well as on glycoproteins. Total lipids were extracted from Tic cells by chloroform/methanol (2:1 v/v) and then by chloroform/methanol/water (1:2:0.8 v/v). The extracts were subjected to TLC blotting with R-10G and the epitope was visualized with a chemiluminescent kit as described for glycoproteins. No R-10G positive component was detected under the conditions tested, in which the SSEA-4 epitope was clearly visualized, indicating that essentially all the R-10G epitopes were expressed on glycoproteins (data not shown).

Finally, the epitopes defined by the R-10G antibody differ from those recognized by the other human iPS/ES cell-specific antibodies and from other keratan sulfate-recognizing antibodies that had been described and provide a new marker for studying the roles of glycans on the surface of hiPS/ES cells in the maintenance of self-renewal and pluripotency and during the process of differentiation, but also as a potent tool for the evaluation and standardization of hiPS cells with different tissue origins and different histories in regenerative medicine. Furthermore, the R-10G antibody might be useful in studies of cancer biology, since the lack of the R-10G epitope on tumor cell surfaces may be somehow relevant to the aberrant properties of tumor cells.

Materials and methods

Materials

Antibodies. Anti-human TRA-1-60 (clone # TRA-1-60, mouse IgM), anti-human TRA-1-81 (clone # TRA-1-81, mouse IgM) and anti-human/mouse SSEA-4 (clone # MC813, mouse IgG3) antibodies were obtained from Santa Cruz Biotechnology (Santa Cruz, CA), and anti-human/mouse SSEA-1 (clone # MC480, mouse IgM), and anti-human/mouse SSEA-3 (clone # MC631, rat IgM) antibodies were obtained from R&D Systems (Minneapolis, MN). Anti-keratan sulfate antibodies, clone # 5D4 (mouse IgG1) and clone # BCD4 (mouse IgG1) were obtained from Seikagaku Biobusiness (Tokyo, Japan).

Glycosaminoglycans. Keratan sulfate from bovine cornea, keratan sulfate from shark cartilage, hyaluronic acid from pig skin, chondroitin from shark cartilage, chondroitin sulfate from whale cartilage, chondroitin sulfate from the spinal column of *Acipenser medirostris*, chondroitin sulfate B from pig skin, chondroitin sulfate C from shark cartilage, chondroitin sulfate D from shark cartilage, chondroitin sulfate E from squid cartilage and heparan sulfate from bovine kidney were obtained from Seikagaku Biobusiness.

Enzymes. PNGase F (recombinant protein from *Escherichia coli*) was obtained from Roche Diagnostics GmbH (Mannheim, Germany), neuraminidase (*Arthrobacter ureafaciens*) from Nacalai Tesque (Kyoto, Japan), neuraminidase (*Vibrio cholerae*) from Roche Diagnostics GmbH, α1–3/4 fucosidase from Takara Bio (Shiga, Japan), α1–2 fucosidase from New England Biolabs (Ipswich, MA). Chondroitinase ABC (*Proteus vulgaris*), a heparinase mix (a mixture of heparinase, heparitinase I and heparitinase II), keratanase (*Pseudomonas* sp.), keratanase II (*Bacillus* sp.) and endo-β-galactosidase (*Escherichia freundii*) were from Seikagaku Biobusiness. Pronase (*Streptomyces griseus*) was obtained from Merck Millipore (Billerica, MA).

Cells and cell culture. HiPS cell lines: Tic (JCRB1331) and Squeaky (JCRB1329), which were generated from MRC-5 (Toyoda et al. 2011), human embryonic lung fibroblasts, by transduction of four defined factors: Oct3/4, Sox2, Klf4 and c-Myc (Takahashi et al. 2007), were obtained from the Japanese Collection of Research Bioresources (JCRB), National Institute of Biomedical Innovation (Osaka, Japan). 201B7 were provided by the Center for iPS Cell Research and Application (CiRA), Kyoto University (Kyoto, Japan). Human ES cell lines, H9 (WA09), were obtained from the Wisconsin International Stem Cell (WISC) Bank, WiCell (Madison, WI), and KhES-3 was provided by the Institute for Frontier Medical Sciences, Kyoto University (Kyoto, Japan). These cells were maintained in KSR-based medium that consisted of KNOCKOUT DMEM/F-12 (400 mL, Invitrogen-Life Technologies, Carlsbad, CA), MEM nonessential amino acids solution (4.0 mL, Invitrogen-Life Technologies), 200 mM L-glutamine (5.0 mL), KNOCKOUT Serum Replacement (100 mL, Invitrogen-Life Technologies), 55 mM 2-mercaptoethanol (0.925 mL) and human basic fibroblast growth factor (bFGF, Sigma-Aldrich, St. Louis, MO) on mitomycin C-inactivated mouse embryonic fibroblasts (MEF, Merck Millipore), in 25 cm^2 flask (Corning, Corning, NY) at 37°C/5% CO_2. Human EC cell line 2102Ep was a generous gift from Prof. Peter Andrews (University of Sheffield) to National Institute of Biomedical Innovation (NIBIO), and NCR-G3 (JCRB1168) was obtained from JCRB. MRC-5 (JCRB9008), a fibroblast-like cell line derived from human lung tissue of a 14-week-old male fetus, was obtained from JCRB. H9 and 2102Ep were cultured only in NIBIO following the Guidelines for Derivation and Utilization of hES Cells of the Ministry of Education, Culture, Sports, Science and Technology of Japan. Furthermore, the study was approved by Independent Ethics Committee of NIBIO. A human tissue array was obtained from BioChain Institution, Inc. (Hayward, CA).

Preparation of monoclonal antibodies recognizing hiPS cells

Preparation of hiPS cells for immunization and screening. An hiPS cell line, Tic, was used as the immunogenic antigen and also as the screening probe. Tic cells cultured in KSR-based medium on MEF were then transferred to a growth factor defined serum-free culture medium hESF9, described previously (Furue et al. 2008). HESF9 medium comprised ESF basal medium without HEPES with L-ascorbic acid 2-phosphate (hESF-grow, Cell Science and Technology Institute, Sendai, Japan) (Furue et al. 2005) supplemented with six-factors (human recombinant insulin, human apotransferrin, 2-mercaptoethanol, 2-ethanolamine, sodium selenite and oleic acid conjugated with fatty acid-free bovine serum albumin (FAF-BSA)), heparin sulfate sodium salt and human bFGF. After culturing at 37°C for 2 days, the undifferentiated hiPS cells ($3 \times 10^5 \sim 1 \times 10^6$ cells/25 cm^2 flask) were harvested by treatment with 0.1% ethylenediaminetetraacetic acid (EDTA)-4Na/phosphate-buffered saline (PBS), washed with PBS and stored at −80°C until just before use as the immunogen. For screening, the cells, which had been incubated with ROCK inhibitor (10 μM, Y27632; Wako Pure Chemical Industries, Osaka, Japan) (Watanabe et al. 2007) for 1 h, were harvested with ACCUTASE™ (1 mL; Merck Millipore), washed with KSR-based medium, resuspended in hESF9 medium and then seeded on fibronectin-coated 96-well plates (5×10^3 cells/well; BD, Franklin Lakes, NJ). After 4 days of culture, cells were fixed with 1% acetic acid/ethanol (100 μL/well) for 10 min at room temperature. After washing with PBS, the plates were stored at −80°C until just before use.

Immunization. Two different protocols were used for the immunization of mice with hiPS cells. In protocol A, freeze-thawed Tic cells (1.5×10^7 cells in 0.5 mL PBS) were emulsified with an equal volume of Freund's Complete Adjuvant (FCA, Thermo Fisher Scientific, Rockford, IL), and then injected into three 8-week-old female C57BL/6 mice (200 μL/mice) intraperitoneally on Day 0, followed by a booster injection on Day 25, and the mice were sacrificed on Day 28. In protocol B, an FCA emulsion of Tic cells was injected subcutaneously into three mice (200 μL/mice) and the mice were sacrificed after 2 weeks.

Cell fusion and cloning. Lymphocytes from the spleens of the protocol A mice and lymph nodes from the protocol B mice were mixed and fused with P3U1 mouse myeloma cells using polyethylene glycol. Fused cells were seeded onto ten 96-well tissue culture plates, and hybridomas were selected by adding the hybridoma medium (S-Clone cloning medium CM-B containing hypoxanthine, aminopterin and thymidine (HAT); Sanko Junyaku, Tokyo, Japan). On Day 7 after plating, the first screening was performed using Tic cell-fixed plates. The culture supernatant from each hybridoma was added to Tic cell-fixed screening plates, which had been pretreated with a blocking solution containing 0.1% H_2O_2 (Blocker Casein; Pierce-Thermo Fisher Scientific) overnight. The hybridoma culture supernatant was incubated on the cell plates at room temperature for 2 h. After washing the plates with PBS, 1:2000-diluted horseradish peroxidase (HRP)-conjugated

anti-mouse IgG (Takara Bio) was added to each well, followed by incubation for 1 h. After final washing, 3,3′-diaminobenzidine (DAB) (Metal Enhanced DAB Substrate Kit (Pierce-Thermo Scientific)) was added to the plates and coloring was allowed to proceed for 10–15 min, followed by observation of the stained plates under a light microscope (Olympus IX 7, Olympus, Tokyo, Japan). The hiPS-positive antibody-producing hybridomas were then subjected to the second cell screening, in which human hEC cells (2102Ep), human fibroblasts (MRC-5) and MEF cells were used as probes as well as hiPS cells (Tic). The isotypes of antibodies were examined by using a mouse monoclonal antibody isotyping test kit (AbD Serotec, Kidlington, UK).

Purification of the R-10G antibody from mouse ascites fluid. The R-10G hybridoma cell line was injected intraperitoneally into pristane-treated SCID mice (CB-17/Icr-scid Jcl). Two weeks later, the ascites fluid (2.5 mL) was collected from the mice and applied to a Protein A-Sepharose column (1 × 6.0 cm) (GE Healthcare, Buckinghamshire, UK). The R-10G antibody bound to the column in 1.5 M glycine-NaOH buffer, pH 8.9/3 M NaCl was eluted with 0.1 M citric acid-phosphate buffer, pH 4.0. The eluate containing the R-10G antibody (IgG1) was immediately neutralized to pH 7–8 by adding 3 M Tris–HCl buffer, pH 9.0.

Immunocytochemistry

Imaging analysis. Cells seeded onto 24-well plates were fixed in 4% paraformaldehyde (PFA) at room temperature for 15 min, blocked with 3% fetal bovine serum (FBS) (ES cell-qualified; Invitrogen-Life Technologies)/PBS for 1 h and then incubated with primary antibodies (R-10G (10 μg/mL), TRA-1-60 (2 μg/mL), TRA-1-81 (2 μg/mL), SSEA-1 (5 μg/mL), SSEA-3 (5 μg/mL) and SSEA-4 (2 μg/mL)) at 4°C overnight. After washing with PBS three times each for 5 min, localization of antibodies was visualized by incubation with Alexa Fluor 647-conjugated chicken anti-mouse IgG (Invitrogen-Life Technologies) as the second antibody at room temperature for 1 h, followed by fixing the cells with 0.1%Triton-X100/4%PFA and then staining with Hoechst 33342 (1:5000 in PBS, Dojindo Laboratories, Kumamoto, Japan). The cells were imaged with an InCell Analyzer 2000 (GE Healthcare, Buckinghamshire, UK) and quantitated with Developer Toolbox ver1.8.

Laser confocal scanning microscopy. Cells were seeded with MEF onto gelatin-coated 4-well plastic chamber (Millipore EZ slides (Millipore, Billerica, MA)). After 3–5 days of culture, the cells were fixed in 4% PFA at room temperature for 10 min, blocked with 3% FBS/PBS for 1 h and then incubated with R-10G (10 μg/mL, as the first primary antibody) at 4°C overnight. After washing with 0.1% PBS three times, the cells were incubated with Alexa Fluor 488-conjugated goat anti-mouse IgG1 as the secondary antibody in 1% FBS/PBS at room temperature for 30–60 min. For double staining with the second primary antibody (TRA-1-60 or TRA-1-81, 2 μg/mL), cells were washed and blocked in the same way as described above and then incubated with the second primary antibody at 4°C overnight. Then, the cells were incubated with Alexa Fluor 555-conjugated goat anti-mouse IgM as the secondary antibody as described above. After washing with 0.1% FBS/PBS three times, the cells were fixed with 0.1% Triton X-100/4% PFA at room temperature for 10 min, followed by staining with TO-PRO3 (1:500 in PBS, Invitrogen-Life Technologies) and monitored under a confocal laser scanning microscope FV1000 (Olympus, Tokyo, Japan).

Isolation of R-10G antigens from hiPS cells

Human iPS cell lysates were prepared by dissolving Tic cells (1.25 mg protein/1 × 10^7 cells, as determined with a Micro BCA protein assay kit (Pierce-Thermo Scientific)) in the complete RIPA buffer (0.5 mL) under sonication. This buffer consists of RIPA lysis buffer (6 mM Tris–HCl, pH 8.0, 1% Nonidet P-40, 0.5% sodium deoxycholate, 0.1% SDS, 0.004% sodium azide), protease inhibitor cocktail, 2.5 mM PMSF and 1 mM sodium orthovanadate (Santa Cruz Biotechnology). The lysate was centrifuged to remove insoluble residues and the supernatant was applied to an R-10G-Sepharose 4B column (gel volume, 0.4 mL), which had been prepared by coupling R-10G (4 mg protein) to BrCN-activated Sepharose 4B (1.0 mL; GE Healthcare) in 0.1 M $NaHCO_3$ buffer, pH 8.3/0.5 M NaCl according to the manufacturer's instructions. After washing the column with the complete RIPA lysis buffer, the protein bound to the column was eluted with an eluting buffer consisting of RIPA buffer (1:10 diluted), protease inhibitor cocktail, PMSF, sodium orthovanadate and 0.1 M diethylamine (pH 11.5). The eluate containing the R-10G antigen was immediately neutralized by adding 1 M Tris–HCl buffer, pH 6.8. In some experiments, the R-10G-Sepharose 4B column was washed with 0.1% Nonidet P-40/20 mM Tris–HCl, pH 7.4/150 mM NaCl, and the protein bound to the column was eluted with 0.1% Nonidet P-40/10 mM Tris–HCl, pH 7.4/150 mM NaCl/0.1 M diethylamine, pH 11.5.

SDS-PAGE and western blotting

SDS–PAGE and western blotting were performed according to the methods of Laemmli (1970) and Towbin et al.(1992). Briefly, samples were resolved by electrophoresis on a 4–15% gradient SDS-polyacrylamide gel (Mini-PROTEAN TGX-gel; Bio-Rad Laboratories, Hercules, CA) under nonreducing conditions unless otherwise stated, followed by either western blotting or protein staining. For western blotting, resolved proteins were transferred to Immobilon Transfer membranes (Merck Millipore), followed by immunoblot detection with R-10G (3 μg/mL), TRA-1-81 (1 μg/mL) or TRA-1-60 (1 μg/mL). For visualization, a chemiluminescent substrate kit (Pierce-Thermo Scientific) was used with HRP-conjugated rabbit anti-mouse immunoglobulin (Dako Cytomation, Denmark A/S), followed by analysis with a Lumino-Image Analyzer, Las 4000 mini (GE Healthcare). Protein was stained with Coomassie brilliant blue G-250 (Gel Code Blue; Invitrogen-Life Technologies).

Identification of the R-10G antigen protein

Following SDS–PAGE, gels were stained with SYPRO Ruby Protein Gel Stain (Invitrogen-Life Technologies), and protein bands corresponding to the western blotting bands were

excised from the gel and subjected to *in gel* trypsin digestion. The peptides extracted from the gel pieces were analyzed by LC/MS/MS using a liquid chromatography instrument (Paradigm MS4 HPLC system; Michrom Bioresources, Auburn, CA) equipped with a linear ion trap type mass spectrometer (LTQ; Thermo Fisher Scientific, Waltham, MA). A reversed-phase column (L-column Micro; 150 × 0.075 mm, 3 μm; Chemicals Evaluation and Research Institute, Tokyo, Japan) was used as the analytical column, the eluents being 2% CH_3CN containing 0.1% formic acid (Pump A) and 90% CH_3CN containing 0.1% formic acid (Pump B). The peptides were eluted at a flow rate of 300 nL/min with a gradient of 2–65% of B buffer in 50 min. Data-dependent MS/MS acquisition was performed for the most intense ions as precursors. The spectrum data obtained on LC/MS/MS were subjected to database search analysis with the TurboSEQUEST algorithm (BioWorks 3.1; Thermo Fisher Scientific) by using the UniProt database. The static modification of carboxymethylation (58.0 u) at Cys was used as the modified parameters for database search analysis. The SEQUEST criterion, known as Xcorr vs. Charge State, was set to 1.5(+1), 2.0(+2), 2.5(+3) and 3.0 (+4) for the protein identifications.

Glycosidase digestions for western blotting

The reaction mixtures consisting of the cell lysates (~12 μg protein, corresponding to 1×10^5 cells) or the R-10G antigen (corresponding to $\sim 1 \times 10^5$ cells) in complete RIPA buffer were digested with various glycosidases under the conditions given below, and the digests were subjected to SDS–PAGE and western blotting. In some experiments, when the solvent for R-10G antigens (RIPA buffer) inhibited the intended enzyme activity, the RIPA buffer was replaced with 0.1% Nonidet P-40/10 mM Tris–HCl, pH 7.4/150 mM NaCl by using an R-10G-Sepharose 4B column (gel volume; 0.4 mL). For chondroitinase ABC digestion, the R-10G antigen was digested with 2 mU of chondroitinase ABC in 20 μL of 50 mM Tris-acetate buffer, pH 8.0, at 37°C for 18 h. For heparinase mix digestion, the R-10G antigen was digested with 6 mU of heparinase mix in 17 μL of 30 mM sodium acetate buffer, pH 7.0, containing 3 mM calcium acetate, at 37°C for 18 h. For keratanase digestion, the R-10G antigen was digested with 1.7 mU of keratanase in 20 μL of 25 mM Tris–HCl buffer, pH 7.4, at 37°C for 18 h. For keratanase II digestion, the R-10G antigen was digested with 0.5–10 mU of keratanase II in 20 μL of 10 mM sodium acetate buffer, pH 6.0, at 37°C for 18 h. For endo-β-galactosidase digestion, the R-10G antigen was digested with 2 mU of endo-β-galactosidase in 20 μL of 20 mM sodium acetate buffer, pH 5.8, at 37°C for 18 h. At the end of these digestions, the incubation mixtures were boiled for 3 min. For PNGase F digestion, Tic cell lysates or the R-10G antigen was heated in a solution consisting of 0.2% Nonidet P-40, 1% SDS, 50 mM 2-mercaptoethanol and 50 mM Tris–HCl buffer, pH 8.2, at 100°C for 5 min. An aliquot of the denatured proteins dissolved in a solution consisting of 0.15% Nonidet P-40, 3.6% octylglucoside, 2 mM EDTA, 63 mM Tris–HCl, pH 8.2 and 0.03% PMSF was digested with 2.0 U of PNGase F at 37°C for 18 h. For digestion with neuraminidase from *Arthrobacter ureafaciens*, the R-10G antigen was digested with 3.75 and 37.5 mU of the enzyme in 30 μL of 0.25 M sodium acetate buffer, pH 4.5, at 37°C for 18 h. For digestion with neuraminidase from *Vibrio cholerae* neuraminidase, the R-10G antigen was digested with 15 mU of the enzyme in 30 μL of 25 mM sodium acetate buffer, pH 5.5, containing 50% PIPA buffer, 77 mM NaCl, 4.5 mM $CaCl_2$ and 0.01% BSA, at 37°C for 18 h. For α1–3/4 fucosidase digestion, the R-10G antigen was digested with 15 μU of α1–3/4 fucosidase in 25 μL of 54 mM potassium phosphate buffer, pH 5.4, containing 0.15% Nonidet P-40, 480 mM $(NH_4)_2SO_4$ and 60 mM NaCl, at 37°C for 18 h. For α1–2 fucosidase digestion, the R-10G antigen was digested with 0.33 U or 2.0 U of α1–2 fucosidase in 10 μL of 50 mM sodium citrate buffer, pH 6.0, containing 0.2% Nonidet P-40, 100 mM NaCl and 0.01% BSA, at 37°C for 18 h.

Isolation of R-10G epitope glycopeptides from the R-10G antigen

The R-10G antigen (~14 μg protein derived from 3×10^7 Tic cells) was digested with pronase (1.4 μg) in 600 μL of 0.1 M borate buffer, pH 8.0, containing 10 mM calcium acetate and 0.04% NaN_3, at 37°C for 72 h. The digest was applied to a column of Sephadex 25 (1 × 17.5 cm), which had been equilibrated and eluted with 10 mM NH_4HCO_3, pH 8.0, to separate glycopeptides from small-size amino acids and peptides. The collected glycopeptides were applied to an R-10G-Sepharose 4B Column (gel volume; 0.4 mL), which had been equilibrated with 50 mM Tris–HCl buffer, pH 7.4, containing 150 mM NaCl. After washing the column with the equilibrium buffer, the glycopeptides bound to the column were eluted with 0.1 M diethylamine (pH 11.5) containing 150 mM NaCl. The eluate containing R-10G epitope glycopeptides was immediately neutralized by adding 1 M Tris–HCl buffer, pH 6.8. The passthrough fraction was collected as nonepitope glycopeptides and the bound fraction was collected as epitope glycopeptides.

Carbohydrate analyses of the R-10G antigen and the glycopeptides obtained therefrom

Neutral sugars were determined according to the procedures described previously (Terada et al. 2005). Briefly, samples were subjected to gas-phase hydrolysis in 4 N HCl and 4 N trifluoroacetic acid (50:50, v/v) 100°C for 4 h. The hydrolysates were reductively aminated with 2-aminopyridine (PA). Analysis of PA-monosaccharides was carried out essentially according to the method described by Suzuki et al. (1991). Sialic acid was determined according to the procedures described previously (Terada et al. 2005). Briefly, sialic acid was liberated from oligosaccharides by heating a sample in 0.1N H_2SO_4 at 80°C for 1.5 h and the liberated sialic acid was labeled with 1,2-diamino-4,5-methylenedioxybenzene (DMB) and quantitated by a fluorometric high-performance liquid chromatography (HPLC) method according to the method of Ito et al. (2002) on a C18 column. The amino sugars were determined according to the procedures described previously (Toyoda et al. 1998). Briefly, samples were subjected to hydrolysis in 6N HCl at 100°C for 2.5 h. Amino sugars released on hydrolysis were separated on a TSKgel

SCX column (4.6 mm i.d. × 150 mm) and eluted with 0.35 M borate/NaOH buffer (pH 7.6) at 60°C, high sensitivity being achieved by post-column reaction with 1% 2-cyanoacetamide. The oligosaccharides released from keratan sulfates on keratanase II digestion were separated with a reversed-phase ion-pair HPLC system using the fluorometric post-column detection, and the degree of sulfation was determined according to the previous procedures (Oguma et al. 2001) and a separate manuscript in preparation by Hirose et al. (in preparation).

Characterization of R-10G epitopes by means of ELISA

GAGs (10 mg/mL in 2-morpholinoethanesulfonic acid (MES) (Wako Pure Chemical Industries) buffer, pH 5.5) (1 mL) and the biotinylation reagent (50 mM EZ-link Hydrazide-Biotin (Pierce-Thermo Scientific) in dimethyl sulfoxide (DMSO) (Sigma-Aldrich)) (25 μL) were mixed, and then the condensing agent (100 mg/mL in MES buffer, pH 5.5, 1-ethyl-3-(3-dimethylaminopropyl) carbodimide-HCl (EDC), (Pierce-Thermo Scientific)) (12.5 μL) was added, followed by incubation overnight at room temperature. The biotinylated GAGs were dialyzed and stored at −20°C until needed for the ELISA assay. The streptavidin (20 μg/mL, Vector Laboratories, Burlingame, CA) (50 μL/well) was immobilized on an ELISA 96-well plate (Nalgene Nunc) overnight at 4°C. To the streptavidin-coated wells, the blocking solution (5-fold dilution, Applie Block, Seikagaku Biobusiness) (250 μL/well) was added, followed by incubation at room temperature for 2 h. After washing the wells with T-Tris-buffered saline (TBS) buffer (50 mM Tris–HCl, pH 7.5, 0.15%NaCl, 0.05% Tween 20 (Wako Pure Chemical Industries) and 0.1% ProCline 950 (Sigma-Aldrich)), the biotinylated GAGs (1 μg/mL, 100 μL) were added, followed by incubation for 30 min at room temperature. After washing the wells with T-TBS buffer, 100 μL of R-10G (1.0 μg/mL) or 5D4 (0.008 μg/mL) was added to the GAG-coated well, followed by incubation at room temperature for 1 h. After washing the wells with T-TBS buffer, the amounts of R-10G and 5D4 bound to the GAGs were determined by incubation with 100 μL of HRP-labeled second antibody (polyclonal goat anti-mouse immunoglobulins/HRP; Dako Cytomation) (0.5 μg/mL) and 100 μL of TMB (3,3′,5,5′-tetramethyl benzidine, BioFX). IgG1 from murine myeloma cells (1.0 μg/mL; Sigma-Aldrich) was used as a negative control. For inhibition experiments, increasing amounts of keratan sulfate (up to 1.0 μg/mL) isolated from bovine cornea or a high-sulfated keratan sulfate isolated from shark cartilage (Kerato polysulfate-1, (KPS-1)) (Furuhashi 1961) were added to the assay system composed of the biotinylated keratan sulfate from bovine cornea on a well plate and the assay was carried out as described above. For enzymatic modifications, the biotinylated keratan sulfate (20 μg/mL, 100 μL) was treated with keratanase (20 mU/mL, 100 μL) or keratanase II (20 mU/mL, 100 μL) at 37°C overnight, and the products were fixed to a streptavidin-coated well plate, and the binding activities of R-10G (1 μg/mL) and 5D4 (0.008 μg/mL) as to the residual oligosaccharide moieties on the biotinylated keratan sulfate were determined as described above.

All of the sugar residues have the D-configuration except fucose, which has the L-configuration.

Funding

This work was supported by Grants-in-Aid for Scientific Research B-20370052 (to T.K.), C-24570171 (to T.K.) and C-20590074 (to N.K.), for Young Scientists Start-up 20890255 (to M.N.), a Grant-in-Aid for the Japan Society for the Promotion of Science (JSPS) Fellows 22-9530 (to M.N.) from JSPS, a Grant-in-Aid for Scientific Research on Innovative Areas 24110517 (to T.K.) from the Ministry of Education, Culture, Sports, Science, and Technology of Japan, Grants from the Ministry of Health, Labor and Welfare of Japan (to M.K.F. and T.K.) and by the R-GIRO (Ritsumeikan Global Innovation Research Organization) Program (to H.T.).

Acknowledgements

We thank Tomoko Tominaga and Saori Kamo for the secretarial assistance.

Conflict of interest

M.K.F. is one of the patent holders and inventors of the basal medium: ESF. However, the licensing fee is <$10,000 dollars.

Abbreviations

BSA, bovine serum albumin; DAB, diaminobenzidine; DMB, 1,2-diamino-4,5-methylenedioxybenzene; DMSO, dimethyl sulfoxide; EC, embryonal carcinoma; ELISA, enzyme-linked immunosorbent assay; FAF, fatty acid-free; FBS, fetal bovine serum; FCA, Freund's complete adjuvant; Fuc, fucose; GAG, glycosaminoglycan; Gal, galactose; GalNAc, *N*-acetylgalactosamine, GCTM, germ cell tumor monoclonal; GlcNAc, *N*-acetylglucosamine; HAT, hypoxanthine, aminopterin and thymidine; hEC, human embryonal carcinoma; hES, human embryonic stem; hiPS, human induced pluripotent stem; HPLC, high performance liquid chromatography; HRP, horseradish peroxidase; iPS, induced pluripotent stem; KPS-1, kerato polysulfate-1; KS, keratan sulfate; LC, liquid chromatography; MEF, mouse embryonic fibroblast; MES, morpholinoethanesulfonic acid; MS, mass spectrometry; NIBIO, National Institute of Biomedical Innovation; PA, 2-aminopyridine; PAGE, polyacrylamide gel electrophoresis; PBS, phosphate-buffered saline; PFA, paraformaldehyde; PNGase F, peptide *N*-glycanase F; PODXL, SDS, sodium dodecyl sulfate; podocalyxin; SSEA, stage-specific embryonic antigen; TBS, Tris-buffered saline. TRA, tumor rejection antigen.

References

Adewumi O, Aflatoonian B, Ahrlund-Richter L, Amit M, Andrews PW, Beighton G, Bello PA, Benvenisty N, Berry LS, Bevan S, et al. 2007. Characterization of human embryonic stem cell lines by the International Stem Cell Initiative. *Nat Biotechnol.* 25:803–816.

Andrews PW, Banting G, Damjanov I, Arnaud D, Avner P. 1984. Three monoclonal antibodies defining distinct differentiation antigens associated with different high molecular weight polypeptides on the surface of human embryonal carcinoma cells. *Hybridoma.* 3:347–361.

Andrews PW, Marrink J, Hirka G, von Keitz A, Sleijfer DT, Gonczol E. 1991. The surface antigen phenotype of human embryonal carcinoma cells: Modulation upon differentiation and viral infection. *Recent Results Cancer Res.* 123:63–83.

Badcock G, Pigott C, Goepel J, Andrews PW. 1999. The human embryonal carcinoma marker antigen TRA-1–60 is a sialylated keratan sulfate proteoglycan. *Cancer Res.* 59:4715–4719.

Brandenberger R, Wei H, Zhang S, Lei S, Murage J, Fisk GJ, Li Y, Xu C, Fang R, Guegler K, et al. 2004. Transcriptome characterization elucidates signaling networks that control human ES cell growth and differentiation. *Nat Biotechnol.* 22:707–716.

Brown GM, Nieduszynski IA, Morris HG, Abram BL, Huckerby TN, Block JA. 1995. Skeletal keratan sulphate structural analysis using keratanase II digestion followed by high-performance anion-exchange chromatography. *Glycobiology.* 5:311–317.

Cai J, Chen J, Liu Y, Miura T, Luo Y, Loring JF, Freed WJ, Rao MS, Zeng X. 2006. Assessing self-renewal and differentiation in human embryonic stem cell lines. *Stem Cells.* 24:516–530.

Cooper S, Pera MF, Bennett W, Finch JT. 1992. A novel keratan sulphate proteoglycan from a human embryonal carcinoma cell line. *Biochem J.* 286(Pt 3):959–966.

Fukuda MN, Matsumura G. 1976. Endo-beta-galactosidase of Escherichia freundii. Purification and endoglycosidic action on keratan sulfates, oligosaccharides, and blood group active glycoprotein. *J Biol Chem.* 251:6218–6225.

Furue M, Okamoto T, Hayashi Y, Okochi H, Fujimoto M, Myoishi Y, Abe T, Ohnuma K, Sato GH, Asashima M, et al. 2005. Leukemia inhibitory factor as an anti-apoptotic mitogen for pluripotent mouse embryonic stem cells in a serum-free medium without feeder cells. *In Vitro Cell Dev Biol Anim.* 41:19–28.

Furue MK, Na J, Jackson JP, Okamoto T, Jones M, Baker D, Hata R, Moore HD, Sato JD, Andrews PW. 2008. Heparin promotes the growth of human embryonic stem cells in a defined serum-free medium. *Proc Natl Acad Sci USA.* 105:13409–13414.

Furuhashi T. 1961. Polysulfated mucopolysaccharides of elasmobranch cartilage. *J Biochem.* 50:546–547.

Hirose Y, Kinoshita-Toyoda A, Toyoda H. Microdetermination of keratan sulfate in biological samples by high-performance liquid chromatography with postcolumn fluorometric detection. in preparation.

Ito M, Hirabayashi Y, Yamagata T. 1986. Substrate specificity of endo-beta-galactosidases from Flavobacterium keratolyticus and Escherichia freundii is different from that of Pseudomonas sp. *J Biochem.* 100:773–780.

Ito M, Ikeda K, Suzuki Y, Tanaka K, Saito M. 2002. An improved fluorometric high-performance liquid chromatography method for sialic acid determination: An internal standard method and its application to sialic acid analysis of human apolipoprotein E. *Anal Biochem.* 300:260–266.

Kannagi R, Cochran NA, Ishigami F, Hakomori S, Andrews PW, Knowles BB, Solter D. 1983. Stage-specific embryonic antigens (SSEA-3 and -4) are epitopes of a unique globo-series ganglioside isolated from human teratocarcinoma cells. *EMBO J.* 2:2355–2361.

Kannagi R, Levery SB, Ishigami F, Hakomori S, Shevinsky LH, Knowles BB, Solter D. 1983. New globoseries glycosphingolipids in human teratocarcinoma reactive with the monoclonal antibody directed to a developmentally regulated antigen, stage-specific embryonic antigen 3. *J Biol Chem.* 258:8934–8942.

Kerjaschki D, Sharkey DJ, Farquhar MG. 1984. Identification and characterization of podocalyxin—the major sialoprotein of the renal glomerular epithelial cell. *J Cell Biol.* 98:1591–1596.

Kershaw DB, Beck SG, Wharram BL, Wiggins JE, Goyal M, Thomas PE, Wiggins RC. 1997. Molecular cloning and characterization of human podocalyxin-like protein. Orthologous relationship to rabbit PCLP1 and rat podocalyxin. *J Biol Chem.* 272:15708–15714.

Kershaw DB, Wiggins JE, Wharram BL, Wiggins RC. 1997. Assignment of the human podocalyxin-like protein (PODXL) gene to 7q32-q33. *Genomics.* 45:239–240.

Laemmli UK. 1970. Cleavage of structural proteins during the assembly of the head of bacteriophage T4. *Nature.* 227:680–685.

Mehmet H, Scudder P, Tang PW, Hounsell EF, Caterson B, Feizi T. 1986. The antigenic determinants recognized by three monoclonal antibodies to keratan sulphate involve sulphated hepta- or larger oligosaccharides of the poly(N-acetyllactosamine) series. *Eur J Biochem.* 157:385–391.

Natunen S, Satomaa T, Pitkanen V, Salo H, Mikkola M, Natunen J, Otonkoski T, Valmu L. 2011. The binding specificity of the marker antibodies Tra-1–60 and Tra-1–81 reveals a novel pluripotency-associated type 1 lactosamine epitope. *Glycobiology.* 21:1125–1130.

Nielsen JS, McNagny KM. 2009. The role of podocalyxin in health and disease. *J Am Soc Nephrol.* 20:1669–1676.

Oguma T, Toyoda H, Toida T, Imanari T. 2001. Analytical method for keratan sulfates by high-performance liquid chromatography/turbo-ionspray tandem mass spectrometry. *Anal Biochem.* 290:68–73.

Pera MF, Blasco-Lafita MJ, Cooper S, Mason M, Mills J, Monaghan P. 1988. Analysis of cell-differentiation lineage in human teratomas using new monoclonal antibodies to cytostructural antigens of embryonal carcinoma cells. *Differentiation.* 39:139–149.

Sassetti C, Tangemann K, Singer MS, Kershaw DB, Rosen SD. 1998. Identification of podocalyxin-like protein as a high endothelial venule ligand for L-selectin: Parallels to CD34. *J Exp Med.* 187:1965–1975.

Sassetti C, Van Zante A, Rosen SD. 2000. Identification of endoglycan, a member of the CD34/podocalyxin family of sialomucins. *J Biol Chem.* 275:9001–9010.

Schopperle WM, DeWolf WC. 2007. The TRA-1-60 and TRA-1-81 human pluripotent stem cell markers are expressed on podocalyxin in embryonal carcinoma. *Stem Cells.* 25:723–730.

Shevinsky LH, Knowles BB, Damjanov I, Solter D. 1982. Monoclonal antibody to murine embryos defines a stage-specific embryonic antigen expressed on mouse embryos and human teratocarcinoma cells. *Cell.* 30:697–705.

Sulak O, Cioci G, Delia M, Lahmann M, Varrot A, Imberty A, Wimmerova M. 2010. A TNF-like trimeric lectin domain from *Burkholderia cenocepacia* with specificity for fucosylated human histo-blood group antigens. *Structure.* 18:59–72.

Suzuki J, Kondo A, Kato I, Hase S, Ikenaka T. 1991. Analysis by high-performance anion-exchange chromatography of component sugars as their fluorescent pyridylamino derivatives(analytical chemistry). *Agric Biol Chem.* 55:283–284.

Takahashi K, Tanabe K, Ohnuki M, Narita M, Ichisaka T, Tomoda K, Yamanaka S. 2007. Induction of pluripotent stem cells from adult human fibroblasts by defined factors. *Cell.* 131:861–872.

Tang C, Lee AS, Volkmer JP, Sahoo D, Nag D, Mosley AR, Inlay MA, Ardehali R, Chavez SL, Pera RR, et al. 2011. An antibody against SSEA-5 glycan on human pluripotent stem cells enables removal of teratoma-forming cells. *Nat Biotechnol.* 29:829–834.

Tateno H, Toyota M, Saito S, Onuma Y, Ito Y, Hiemori K, Fukumura M, Matsushima A, Nakanishi M, Ohnuma K, et al. 2011. Glycome diagnosis of human induced pluripotent stem cells using lectin microarray. *J Biol Chem.* 286:20345–20353.

Terada M, Khoo KH, Inoue R, Chen CI, Yamada K, Sakaguchi H, Kadowaki N, Ma BY, Oka S, Kawasaki T, et al. 2005. Characterization of oligosaccharide ligands expressed on SW1116 cells recognized by mannan-binding protein. A highly fucosylated polylactosamine type *N*-glycan. *J Biol Chem.* 280:10897–10913.

Towbin H, Staehelin T, Gordon J. 1992. Electrophoretic transfer of proteins from polyacrylamide gels to nitrocellulose sheets: Procedure and some applications. 1979. *Biotechnology.* 24:145–149.

Toyoda H, Demachi Y, Komoriya S, Furuya N, Toida T, Imanari T. 1998. Characterization and determination of human urinary keratan sulfate. *Chem Pharm Bull (Tokyo).* 46:97.

Toyoda M, Yamazaki-Inoue M, Itakura Y, Kuno A, Ogawa T, Yamada M, Akutsu H, Takahashi Y, Kanzaki S, Narimatsu H, et al. 2011. Lectin microarray analysis of pluripotent and multipotent stem cells. *Genes Cells.* 16:1–11.

Watanabe K, Ueno M, Kamiya D, Nishiyama A, Matsumura M, Wataya T, Takahashi JB, Nishikawa S, Nishikawa S, Muguruma K, et al. 2007. A ROCK inhibitor permits survival of dissociated human embryonic stem cells. *Nat Biotechnol.* 25:681–686.

Wright AJ, Andrews PW. 2009. Surface marker antigens in the characterization of human embryonic stem cells. *Stem Cell Research.* 3:3–11.

Biomaterials 34 (2013) 1781–1789

Contents lists available at SciVerse ScienceDirect

Biomaterials

journal homepage: www.elsevier.com/locate/biomaterials

3D spheroid culture of hESC/hiPSC-derived hepatocyte-like cells for drug toxicity testing

Kazuo Takayama [a,b], Kenji Kawabata [b,c], Yasuhito Nagamoto [a,b], Keisuke Kishimoto [a,b], Katsuhisa Tashiro [b], Fuminori Sakurai [a], Masashi Tachibana [a], Katsuhiro Kanda [d], Takao Hayakawa [e], Miho Kusuda Furue [f,g], Hiroyuki Mizuguchi [a,b,h,*]

[a] Laboratory of Biochemistry and Molecular Biology, Graduate School of Pharmaceutical Sciences, Osaka University, Osaka 565-0871, Japan
[b] Laboratory of Stem Cell Regulation, National Institute of Biomedical Innovation, Osaka 567-0085, Japan
[c] Laboratory of Biomedical Innovation, Graduate School of Pharmaceutical Sciences, Osaka University, Osaka 565-0871, Japan
[d] Pharma Business Project, Corporate Projects Center, Corporate Strategy Division, Hitachi High-Technologies Corporation, Ibaraki 312-8504, Japan
[e] Pharmaceutical Research and Technology Institute, Kinki University, Osaka 577-8502, Japan
[f] Laboratory of Embryonic Stem Cell Cultures, Department of Disease Bioresources Research, National Institute of Biomedical Innovation, Osaka 567-0085, Japan
[g] Department of Embryonic Stem Cell Research, Field of Stem Cell Reseach, Institute for Frontier Medical Sciences, Kyoto University, Kyoto 606-8507, Japan
[h] The Center for Advanced Medical Engineering and Informatics, Osaka University, Osaka 565-0871, Japan

ARTICLE INFO

Article history:
Received 11 September 2012
Accepted 20 November 2012
Available online 8 December 2012

Keywords:
Hepatocyte-like cell
Human ES cell
Human iPS cell
Nanopillar plate
Drug screening

ABSTRACT

Although it is expected that hepatocyte-like cells differentiated from human embryonic stem (ES) cells or induced pluripotent stem (iPS) cells will be utilized in drug toxicity testing, the actual applicability of hepatocyte-like cells in this context has not been well examined so far. To generate mature hepatocyte-like cells that would be applicable for drug toxicity testing, we established a hepatocyte differentiation method that employs not only stage-specific transient overexpression of hepatocyte-related transcription factors but also a three-dimensional spheroid culture system using a Nanopillar Plate. We succeeded in establishing protocol that could generate more matured hepatocyte-like cells than our previous protocol. In addition, our hepatocyte-like cells could sensitively predict drug-induced hepatotoxicity, including reactive metabolite-mediated toxicity. In conclusion, our hepatocyte-like cells differentiated from human ES cells or iPS cells have potential to be applied in drug toxicity testing.

1. Introduction

Hepatocyte-like cells that are generated from human embryonic stem cells (hESCs) [1] or human induced pluripotent stem cells (hiPSCs) [2] are expected to be used in drug screening instead of primary (or cryopreserved) human hepatocytes (PHs). We recently demonstrated that stage-specific transient transduction of transcription factors, in addition to treatment with optimal growth factors and cytokines, is useful for promoting hepatic differentiation [3–6]. The hepatocyte-like cells, which have many hepatocyte characteristics (the abilities to uptake low-density lipoprotein and Indocyanine green, store glycogen, and synthesize urea) and drug metabolism capacity, were generated from hESCs/hiPSCs by combinational transduction of FOXA2 and HNF1α [6]. However, further maturation of the hepatocyte-like cells is required because their hepatic characteristics, such as drug metabolism capacity, are lower than those of PHs [6].

To promote further maturation of the hepatocyte-like cells, we subjected them to three-dimensional (3D) spheroid cultures. It is known that various 3D culture conditions (such as Algimatrix scaffolds [7], cell sheet technology [8], galactose-carrying substrata [9], and basement membrane substratum [10]) are useful for the maturation of the hepatocyte-like cells. Nanopillar Plate technology [11] used in the present study makes it easy to control the configuration of the spheroids. The Nanopillar Plate has an arrayed μm-scale hole structure at the bottom of each well, and nanopillars were aligned further at the bottom of the respective holes. The seeded cells evenly drop into the holes, then migrate and aggregate on top surface of the nanopillars, thus likely to form the uniform spheroids in each hole. Not only 3D spheroid cultures [12] but also Matrigel overlay cultures [13] are useful for maintaining the hepatocyte characteristics of PHs. Therefore, we employed both 3D

* Corresponding author. Laboratory of Biochemistry and Molecular Biology, Graduate School of Pharmaceutical Sciences, Osaka University, 1-6 Yamadaoka, Suita, Osaka 565-0871, Japan. Tel.: +81 6 6879 8185; fax: +81 6 6879 8186.
E-mail address: mizuguch@phs.osaka-u.ac.jp (H. Mizuguchi).

0142-9612/$ – see front matter © 2012 Elsevier Ltd. All rights reserved.
http://dx.doi.org/10.1016/j.biomaterials.2012.11.029

spheroid culture and Matrigel overlay culture systems to promote hepatocyte maturation of the hepatocyte-like cells.

The hepatocyte-like cells generated from hESCs/hiPSCs are expected to be used in drug development. To the best of our knowledge, however, few studies have tried to predict widespread drug-induced cytotoxicity *in vitro* using the hepatocyte-like cells. To precisely determine the applicability of the hepatocyte-like cells to drug screening, it is necessary to investigate the responses of these hepatocyte-like cells to many kinds of hepatotoxic drugs.

In this study, 3D spheroid and Matrigel overlay cultures of the hepatocyte-like cells were performed to promote hepatocyte maturation. The gene expression analysis of cytochrome P450 (CYP) enzymes, conjugating enzymes, hepatic transporters, and hepatic nuclear receptors in the 3D spheroid-cultured hESC- or hiPSC-derived hepatocyte-like cells (3D ES-hepa or 3D iPS-hepa), were analyzed. In addition, CYP induction potency and drug metabolism capacity were estimated in the 3D ES/iPS-hepa. To determine the suitability of these cells for drug screening, we examined whether the drug-induced cytotoxicity is induced by treatment of various kinds of hepatotoxic drugs in 3D ES/iPS-hepa.

2. Materials and methods

2.1. hESCs and hiPSCs culture

A hESC line, H1 and H9 (WiCell Research Institute), was maintained on a feeder layer of mitomycin C-treated mouse embryonic fibroblasts (Millipore) with Repro Stem medium (Repro CELL) supplemented with 5 ng/ml fibroblast growth factor 2 (FGF2) (Sigma). Both H1 and H9 were used following the Guidelines for Derivation and Utilization of Human Embryonic Stem Cells of the Ministry of Education, Culture, Sports, Science and Technology of Japan and furthermore, and the study was approved by Independent Ethics Committee.

Three human iPSC lines were provided from the JCRB Cell Bank (Tic, JCRB Number: JCRB1331; Dotcom, JCRB Number: JCRB1327; Toe, JCRB Number: JCRB1338) [14,15]. These human iPSC lines were maintained on a feeder layer of mitomycin C-treated mouse embryonic fibroblasts with iPSellon (Cardio) supplemented with 10 ng/ml FGF2. Other three human iPSC lines, 201B6, 201B7 and 253G1 were kindly provided by Dr. S. Yamanaka (Kyoto University) [2]. These human iPSC lines were maintained on a feeder layer of mitomycin C-treated mouse embryonic fibroblasts with Repro Stem supplemented with 5 ng/ml FGF2.

2.2. In vitro differentiation

Before the initiation of cellular differentiation, the medium of hESCs was exchanged into a defined serum-free medium, hESF9, and cultured as previously reported [16]. The differentiation protocol for the induction of definitive endoderm cells, hepatoblasts, and hepatocytes was based on our previous reports with some modifications [3–5,17]. Briefly, in mesendoderm differentiation, hESCs were dissociated into single cells by using Accutase (Millipore) and cultured for 2 days on Matrigel (BD Biosciences) in differentiation hESF-DIF medium which contains 100 ng/ml Activin A (R&D Systems) and 10 ng/ml bFGF (hESF-DIF medium was purchased from Cell Science & Technology Institute; differentiation hESF-DIF medium was supplemented with 10 μg/ml human recombinant insulin, 5 μg/ml human apotransferrin, 10 μM 2-mercaptoethanol, 10 μM ethanolamine, 10 μM sodium selenite, and 0.5 mg/ml bovine fatty acid free serum albumin [all from sigma]). To generate definitive endoderm cells, the mesendoderm cells were transduced with 3000 vector particle (VP)/cell of Ad-FOXA2 for 1.5 h on day 2 and cultured until day 6 on Matrigel in differentiation hESF-DIF medium supplemented with 100 ng/ml Activin A and 10 ng/ml bFGF. For induction of hepatoblasts, the DE cells were transduced with each 1500 VP/cell of Ad-FOXA2 and Ad-HNF1α for 1.5 h on day 6 and cultured for 3 days on Matrigel in hepatocyte culture medium (HCM) (Lonza) supplemented with 30 ng/ml bone morphogenetic protein 4 (BMP4) (R&D Systems) and 20 ng/ml FGF4 (R&D Systems). In hepatic expansion, the hepatoblasts were transduced with each 1500 VP/cell of Ad-FOXA2 and Ad-HNF1α for 1.5 h on day 9 and cultured for 3 days on Matrigel in HCM supplemented with 10 ng/ml hepatocyte growth factor (HGF), 10 ng/ml FGF1, 10 ng/ml FGF4, and 10 ng/ml FGF10 (all from R&D Systems). To perform hepatocyte maturation on Nanopillar Plate (a prototype multi-well culturing plate for spheroid culture developed and prepared by Hitachi High-Technologies Corporation) shown in Fig. 1B, the cells were seeded at 2.5×10^5 cells/cm^2 (Fig. S1) in hepatocyte culture medium (Fig. S2) supplemented with 10 ng/ml HGF, 10 ng/ml FGF1, 10 ng/ml FGF4, and 10 ng/ml FGF10 on day 11. In the first stage of hepatocyte maturation (from day 12 to day 25), the cells were cultured for 13 days on Matrigel in HCM supplemented with 20 ng/ml HGF, 20 ng/ml oncostatin M (OsM), 10 ng/ml FGF4, and 10^{-6} M dexamethasone (DEX). In the second stage of hepatocyte maturation (from day 25 to day 35), Matrigel was overlaid on the hepatocyte-like cells. Matrigel were diluted to a final concentration of 0.25 mg/ml with William's E medium (Invitrogen) containing 4 mM L-glutamine, 50 ug/ml gentamycin sulfate, 1 × ITS (BD Biosciences), 20 ng/ml OsM, and 10^{-6} M DEX. The culture medium was aspirated, and then the Matrigel solution (described above) was overlaid on the hepatocyte-like cells. The cells were incubated overnight, and the medium was replaced with HCM supplemented with 20 ng/ml OsM and 10^{-6} M DEX.

2.3. Adenovirus (Ad) vectors

Ad vectors were constructed by an improved *in vitro* ligation method [18,19]. The human EF-1α promoter-driven LacZ-, FOXA2-, or HNF1α-expressing Ad vectors (Ad-LacZ, Ad-FOXA2, or Ad-HNF1α, respectively) were constructed previously [3,4,20]. All of Ad vectors contain a stretch of lysine residue (K7) peptides in the C-terminal region of the fiber knob for more efficient transduction of hESCs, hiPSCs, and DE cells, in which transfection efficiency was almost 100%, and purified as described previously [3–5]. The vector particle (VP) titer was determined by using a spectrophotometric method [21].

2.4. Flow cytometry

Single-cell suspensions of hESC/hiPSC-derived cells were fixed with 2% paraformaldehyde (PFA) at 4°C for 20 min, and then incubated with the primary antibody (described in Table S1), followed by the secondary antibody (described in Table S1). Flow cytometry analysis was performed using a FACS LSR Fortessa flow cytometer (BD Biosciences).

2.5. RNA isolation and reverse transcription-polymerase chain reaction (RT-PCR)

Total RNA was isolated from hESCs or hiPSCs and their derivatives using ISOGENE (Nippon Gene). cDNA was synthesized using 500 ng of total RNA with a Superscript VILO cDNA synthesis kit (Invitrogen). Real-time RT-PCR was performed with Taqman gene expression assays (Applied Biosystems) or SYBR Premix Ex Taq (TaKaRa) using an ABI PRISM 7000 Sequence Detector (Applied Biosystems). Relative quantification was performed against a standard curve and the values were normalized against the input determined for the housekeeping gene, glyceraldehyde 3-phosphate dehydrogenase (GAPDH). The primer sequences used in this study are described in Table S2.

2.6. Immunohistochemistry

The cells were fixed with 4% PFA. After incubation with 1% Triton X-100, blocking with Blocking One (Nakalai tesque), the cells were incubated with primary antibody (describe in Table S1) at 4°C for over night, followed by incubation with a secondary antibody (described in Table S1) at room temperature for 1 h.

2.7. ELISA

The hESCs or hiPSCs were differentiated into hepatocytes as described in Fig. 1A. The culture supernatants, which were incubated for 24 h after fresh medium was added, were collected and analyzed for the amount of ALB secretion by ELISA. ELISA kits for ALB were purchased from Bethyl. ELISA was performed according to the manufacturer's instructions. The amount of ALB secretion was calculated according to each standard followed by normalization to the protein content per well.

2.8. Urea secretion

The hESCs or hiPSCs were differentiated into hepatocytes as described in Fig. 1A. The culture supernatants, which were incubated for 24 h after fresh medium was added, were collected and analyzed for the amount of urea secretion. Urea measurement kits were purchased from BioAssay Systems. The experiment was performed according to the manufacturer's instructions. The amount of urea secretion was calculated according to each standard followed by normalization to the protein content per well.

2.9. Canalicular secretory assay

At cellular differentiation, the hepatocyte-like cell spheroids were treated with 5 mM choly-lysyl-fluorescein (CLF) (BD Biosciences) for 30 min. The cells were washed with culture medium, and then observed by fluorescence microscope. To inhibit the function of BSEP, the cells were pretreated with Cyclosporin A 24 h before of the CLF treatment.

2.10. Assay for CYP activity and CYP induction

To measure the cytochrome P450 2C9 and 3A4 activity of the cells, we performed lytic assays by using a P450-GloTM CYP2C9 (catalog number; V8791) and

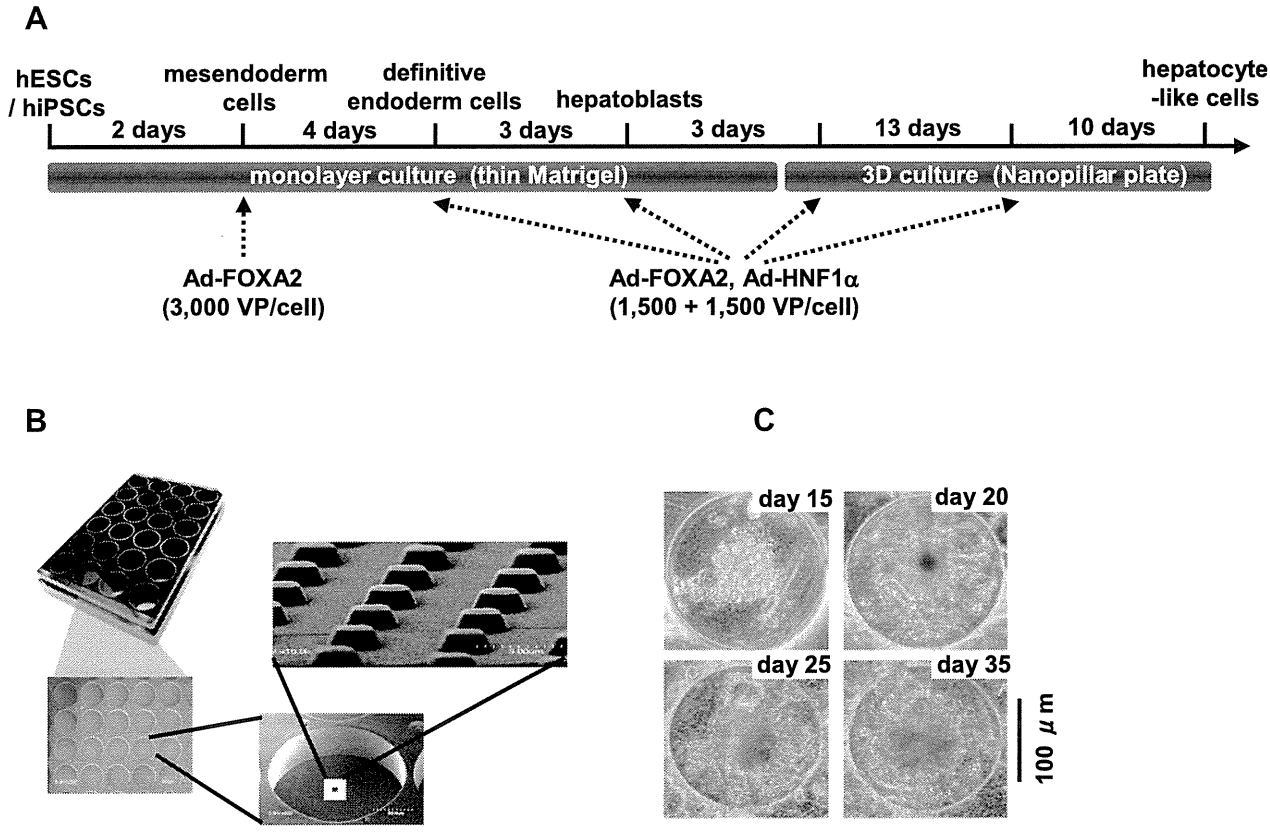

Fig. 1. Hepatocyte-like cells were differentiated from hESCs/hiPSCs by using Nanopillar Plate. (A) The procedure for differentiation of hESCs into 3D ES/iPS-hepa via mesendoderm cells, definitive endoderm cells, and hepatoblasts is presented schematically. In the differentiation, not only the addition of growth factors but also stage-specific transient transduction of both FOXA2- and HNF1α-expressing Ad vector (Ad-FOXA2 and Ad-HNF1α, respectively) was performed. The cellular differentiation procedure is described in detail in the materials and methods section. (B) Photograph display of a 24-well format Nanopillar Plate and its microstructural appearances of the hole and pillar structure. (C) Phase-contrast micrographs of the hESC-hepa spheroids on the Nanopillar Plate are shown. Scale bar represents 100 μm.

3A4 (catalog number; V9001) Assay Kit (Promega), respectively. We measured the fluorescence activity with a luminometer (Lumat LB 9507; Berthold) according to the manufacturer's instructions. The CYP activity was normalized with the protein content per well.

To measure CYP2C9 and 3A4 induction potency, the CYP activity was measured by using a P450-GloTM CYP2C9 and 3A4 Assay Kit, respectively. The cells were treated with rifampicin, which is known to induce both CYP2C9 and 3A4, at a final concentration of 10 μM for 48 h. The cells were also treated with Ketoconazole (Sigma) or Sulfaphenazole (Sigma), which are inhibitors for CYP3A4 or 2C9, at a final concentration of 1 μM or 2 μM, respectively, for 48 h. Controls were treated with DMSO (final concentration 0.1%). Inducer compounds were replaced daily.

2.11. Cell viability tests

Cell viability was assessed by the WST-8 assay kit (Dojindo) in Fig. 2D. After treatment with test compounds, such as Acetaminophen (Wako), Allopurinol (Wako), Amiodaron (Sigma), Benzbromarone (Sigma), Clozapine (Wako), Cyclizine (MP bio), Dantrolene (Wako), Desipramine (Wako), Disufliram (Wako), Erythromycin (Wako), Felbamate (Sigma), Flutamide (Wako), Isoniazid (Sigma), Labetalol (Sigma), Lefunomide (Sigma), Maprotiline (Sigma), Nefazodone (Sigma), Nitrofurantoin (Sigma), Sulindac (Wako), Tacrine (Sigma), Tebinafine (Wako), Tolcapone (TRC), Troglitazone (Wako), and Zafirlukast (Cayman) for 24 h, the cell viability was measured. The cell viability of the 3D iPSC-hepa were assessed by WST-8 assay after 24 h exposure to different concentrations of Aflatoxin B1 (Sigma) and Benzbromarone in the presence or absence of the CYP3A4 or 2C9 inhibitor, Ketoconazole (1 μM) or Sulfaphenazole (10 μM), respectively. The control refers to incubations in the absence of test compounds and was considered as 100% viability value. Controls were treated with DMSO (final concentration 0.1%). ATP assay (BioAssay Systems), Alamar Blue assay (Invitrogen), and Crystal Violet (Wako) staining assay were performed according to the manufacturer's instructions.

2.12. Primary human hepatocytes

Three lots of cryopreserved human hepatocytes (lot Hu8072 [CellzDirect], HC2-14, and HC10-101 [Xenotech]) were used. These three lots of crypreserved human hepatocytes were cultured according to our previous report [5].

2.13. Statistical analysis

Statistical analysis was performed using the unpaired two-tailed Student's *t*-test. All data are represented as means ± SD ($n = 3$).

3. Results

The 3D ES/iPS-hepa were generated from hESCs/hiPSCs as shown in Fig. 1A. Hepatocyte differentiation of hESCs/hiPSCs was efficiently promoted by stage-specific transient transduction of FOXA2 and HNF1α in addition to the treatment with appropriate soluble factors (growth factors and cytokines) [6]. On day 11, the hESC-derived cells were seeded at 2.5×10^5 cells/cm^2 (Fig. S1) on Nanopillar Plate (Fig. 1B), in hepatocyte culture medium (Fig. S2) to promote hepatocyte maturation. In addition, Matrigel was overlaid on the 3D ES-hepa to promote further hepatocyte maturation. The 3D ES-hepa with compact morphology that were adhesive to the substratum and had an optimal size (approximately 100 μm in diameter) were formed by using the Nanopillar Plate (Fig. 1C). The spheroids seem to be stable because they could be cultured for more than 20 days. We have confirmed that more than 90% of the cells that constitute the spheroids were alive, indicating that the necrotic centers are absent.

To investigate whether or not a 3D spheroid culture could promote hepatocyte maturation of the hepatocyte-like cells, various hepatocyte characteristics of the 3D ES/iPS-hepa were compared with those of the monolayer-cultured hESC- or hiPSC-derived hepatocyte-like cells (mono ES-hepa or mono iPS-hepa). The gene expression level of *ALB* peaked on day 20 in the mono ES-hepa, and then it was dramatically decreased after day 25 (Fig. 2A). In contrast, the gene expression level of *ALB* was